

Efficient Discovery of Heterogeneous Quantile Treatment Effects in Randomized Experiments via Anomalous Pattern Detection

Edward McFowland III

Technology Operations and Management
Harvard Business School
Boston, MA 02163, USA

Sriram Somanchi

IT, Analytics, and Operations
University of Notre Dame

Daniel B. Neill

Machine Learning for Good Laboratory
New York University

Abstract

In the recent literature on estimating heterogeneous treatment effects, each proposed method makes its own set of restrictive assumptions about the intervention’s effects and which subpopulations to explicitly estimate. Moreover, the majority of the literature provides no mechanism to identify which subpopulations are the most affected—beyond manual inspection—and provides little guarantee on the correctness of the identified subpopulations. Therefore, we propose Treatment Effect Subset Scan (TESS), a new method for discovering which subpopulation in a randomized experiment is most significantly affected by a treatment. We frame this challenge as a pattern detection problem where we efficiently maximize a nonparametric scan statistic (a measure of the conditional quantile treatment effect) over subpopulations. Furthermore, we identify the subpopulation which experiences the largest distributional change as a result of the intervention, while making minimal assumptions about the intervention’s effects or the underlying data generating process. In addition to the algorithm, we demonstrate that under the sharp null hypothesis of no treatment effect, the asymptotic Type I and II error can be controlled, and provide sufficient conditions for detection consistency—i.e., exact identification of the affected subpopulation. Finally, we validate the efficacy of the method by discovering heterogeneous treatment effects in simulations and in real-world data from a well-known program evaluation study.

1 Introduction

The randomized experiment is employed across many empirical disciplines as an important tool for discovery, by estimating the causal impact of a particular stimulus, treatment or intervention. Moreover, the increasing popularity of large-scale experiments [32] has resulted in a widespread interest in discovering fine-grained truths about experimental units, most prominently in the form of heterogeneous treatment effects (HTE). Discovering heterogeneity can be challenging because there are exponentially many subpopulations—with respect to the number of observable covariates—to consider, potentially resulting in multiple hypothesis testing issues and raising questions of unprincipled post-hoc investigation: searching for a fortuitously statistically significant result [5, 52]. Nevertheless, uncovering affected subpopulations can lead to important scientific progress. In a “step toward a new frontier of personalized medicine” [41], the FDA approved the first race-specific drug, whose impact on African-American subjects was first discovered post-hoc from more general experiments [15, 16]. Conversely, the Perry preschool experiment found significant effects of preschool education on educational and life outcomes [9, 43, 3], while a re-analysis focused on heterogeneity and multiple hypothesis testing concluded that only girls experience these benefits [2]. The original Perry preschool results were fundamental to the creation of the Head Start preschool program [3] a national social program that provides, among other services, early childhood education to low-income children. If large-scale medical and policy decisions are made as a result of such experiments, then it is clear that identifying whether there is heterogeneity in treatment effects should be an integral component of the analysis.

In this work we propose a novel computationally efficient framework—Treatment Effect Subset Scanning (TESS)—for *discovering* which subpopulations in a randomized experiment are the most significantly affected by a treatment. The contributions of this work can be summarized as follows:

- Our TESS algorithm enables efficient discovery of subpopulations where the individuals affected by the treatment have observed outcome distributions that are unexpected given the distributions of their corresponding control groups.
- We formalize the objective of identifying subpopulations with significant distributional treatment effects by developing a new measure and test statistic for heterogeneous quantile treatment effects.
- We provide theoretical results on the detection properties of TESS. When the maximum subpopulation score identified by TESS is used as a test statistic under the sharp null hypothesis of no treatment effect, we demonstrate the conditions under which the Type I (Theorem 2) and Type II (Theorem 3) errors can jointly be controlled asymptotically. Furthermore, we provide sufficient conditions on how “homogeneous” (Theorem 4) and “strong” (Theorem 5) the treatment effect must be across the affected subpopulation, such that the TESS test statistic is maximized at the precisely correct subpopulation. Finally, we show that asymptotically these conditions are met (Theorems 6 and 7), guaranteeing that, in the large-sample limit, TESS will recover the precisely correct subpopulation.
- In the process of developing theory for TESS, we prove results for the general non-parametric scan statistic (NPSS), which has been used in the scan statistics liter-

ature [35, 11]. We are the first to provide theoretical guarantees on the detection behavior of subset scanning algorithms. Furthermore, our theory is derived for the higher dimensional (tensor) context, with nonparametric score functions, and our results directly hold for the lower-dimensional and parametric cases as well.

- Our empirical results (§5.4) provide useful insights to practitioners, revealing a potentially affected subpopulation in the Tennessee STAR study of class size and educational outcomes, who may have benefited from an intervention (the use of a teacher’s aide) that was generally considered ineffective.

These contributions are enabled by structuring the question of causal inference as one of *anomalous pattern detection* and effect maximization, rather than model fitting and risk minimization. In some contexts, the standard approach of learning an overall model of the treatment effect response surface is desirable; however, in many cases, the identification of affected subpopulations is the primary goal and model learning is simply a step toward this goal. For these cases it seems prudent and efficient to circumvent this first step and solve the subpopulation identification problem by framing it as one of pattern or subset discovery. Such a framing has not previously been considered in the literature.

2 Heterogeneous Quantile Treatment Effects

Most contemporary causal methods are estimators for the (conditional) average treatment effects, or CATE, $\tau_{CATE}(x) = \mathbb{E}[Y(1) - Y(0)|X = x]$, which in turn limits empirical studies of treatment effects from considering effects beyond mean shifts [1]. However, social scientists argue that effects can greatly vary along the outcome distribution, and distributional impacts beyond the average effect are critical for policy-makers, across a wide range of social programs [18, 1, 14, 42]. The primary distributional alternative to ATEs has been Quantile Treatment Effects (QTE) and the subsequent conditional QTEs, or CQTE [18, 31, 30, 13] at a given quantile α :

$$\tau_{CQTE_\alpha}(x) = \mathbb{F}_{Y(1)|X=x}^{-1}(\alpha) - \mathbb{F}_{Y(0)|X=x}^{-1}(\alpha), \quad (1)$$

where $\mathbb{F}_{Y(1)|X=x}^{-1}$ and $\mathbb{F}_{Y(0)|X=x}^{-1}$ denote the inverse cumulative distribution functions of the outcome Y , conditional on covariates $X = x$, under the counterfactual assignments to the treatment group ($W = 1$) and control group ($W = 0$) respectively.

In this work, we consider the challenge of *heterogeneous* quantile treatment effects, i.e., **detecting** the existence of a subpopulation S (characterized by a subset of values for each attribute) for which the CQTE is non-zero, at some quantile, even if there is not a significant effect in the overall population. This motivates the need for a measurement of the heterogeneous treatment effect $\tau_{CQTE_\alpha}(S)$ and a corresponding test statistic $F_\alpha(S)$ that can be optimized over both subpopulations S and quantiles α , capturing unknown heterogeneity in both covariates and the treatment effect distribution, respectively. While a simple extension to (1),

$$\max_S \tau_{CQTE}(S) = \max_S \max_\alpha \tau_{CQTE_\alpha}(S) = \max_S \max_\alpha \mathbb{F}_{Y(1)|X \in S}^{-1}(\alpha) - \mathbb{F}_{Y(0)|X \in S}^{-1}(\alpha), \quad (2)$$

may appear to be an attractive alternative, this formulation is inadequate for detecting subpopulations with distributional effects. Note that in (2) the effect is represented by a

difference in scalar summaries of the potential outcome distributions, instead of capturing *full* distributional effect [13, 50]. Moreover, it *first* aggregates $\mathbb{F}_{Y(W)|X=x} \forall x \in S$ to construct $\mathbb{F}_{Y(W)|X \in S}$ and then compares these aggregate conditional distributions, instead of *first* comparing each $\mathbb{F}_{Y(1)|X=x}$ to the corresponding $\mathbb{F}_{Y(0)|X=x} \forall x \in S$ and *then* aggregating.¹ The effect of interest can easily be obfuscated when aggregating before comparing: consider that $Y(W)|X = x$ need not be on the same scale for different $x \in S$. Additionally, (2) tends to be maximized at extreme values $\alpha \approx 0$ and $\alpha \approx 1$ and is thus highly sensitive to outliers, losing power to detect QTEs occurring at non-extreme values of α . Finally, (2) fails to appropriately calibrate the treatment effect across potential subpopulations S of varying sizes, and therefore in (2) the optimal S equates to $\max_{x,\alpha} \tau_{\text{CQTE}_\alpha}(x)$, i.e., a singular covariate profile (see proof in Appendix A). This last issue also arises when maximizing other popular conditional treatment effect estimands in the literature, such as CATE, over subpopulations.

To avoid these limitations, we first recognize that our primary goals are to *test* the null hypothesis

$$\mathbb{F}_{Y(0)|X=x}^{-1}(\alpha) = \mathbb{F}_{Y(1)|X=x}^{-1}(\alpha),$$

for $\alpha \in (0, 1)$ and $\forall x$, and to *detect* subpopulations S for which the two counterfactual outcome distributions differ significantly. An equivalent test is for

$$\mathbb{F}_{Y(1)|X=x}(\mathbb{F}_{Y(0)|X=x}^{-1}(\alpha)) = \mathbb{F}_{Y(1)|X=x}(\mathbb{F}_{Y(1)|X=x}^{-1}(\alpha)) = \alpha.$$

Moreover, re-defining $\tau_{\text{CQTE}_\alpha}(x) = \mathbb{F}_{Y(1)|X=x}(\mathbb{F}_{Y(0)|X=x}^{-1}(\alpha))$ captures the *full* distributional effect (as demonstrated by [13, 50]) prior to aggregation, and is constrained to $(0, 1)$, allowing coherent aggregation and calibration over $x \in S$. More precisely, we can define $\tau_{\text{CQTE}_\alpha}(S) = \sum_{x \in S} \tau_{\text{CQTE}_\alpha}(x) P(X = x | X \in S)$, and then define a test statistic $F_\alpha(S)$ to measure the significance of the divergence between $\tau_{\text{CQTE}_\alpha}(S)$ and α .

Therefore, we can make specific, simple, and testable assumptions about the relationships between each $\mathbb{F}_{Y(0)|X=x}$ and $\mathbb{F}_{Y(1)|X=x}$, under the null and alternative hypotheses, and construct a generalized likelihood ratio test that maximizes detection power for distinguishing these hypotheses:

$$\begin{aligned} H_0 : \tau_{\text{CQTE}_\alpha}(x) &= \alpha \quad \forall x, \alpha \\ H_1(S) : \begin{cases} \exists \beta, \alpha, \text{ with } \beta > \alpha, \text{ s.t.} & \tau_{\text{CQTE}_\alpha}(x) = \beta \quad \forall x \in S, \\ \forall \alpha & \tau_{\text{CQTE}_\alpha}(x) = \alpha \quad \forall x \notin S. \end{cases} \end{aligned} \quad (3)$$

We define $H_1(S)$ as in (3) (with constant $\beta_x = \beta$) because of our interest in detecting subsets S where $\mathbb{F}_{Y(1)|X=x}$ differs *systematically* from $\mathbb{F}_{Y(0)|X=x}$ for $x \in S$, thus grouping together covariate profiles that exhibit similar treatment effects, rather than massively overfitting to individual covariate profiles.² Moreover, if $\mathbb{F}_{Y(1)|X=x} \neq \mathbb{F}_{Y(0)|X=x}$, we know that there exists some α and some subset S such that $\tau_{\text{CQTE}_\alpha}(S) = \beta \neq \alpha$, while if $\mathbb{F}_{Y(1)|X=x} = \mathbb{F}_{Y(0)|X=x}$,

¹When the effects of interest are simply differences in scalar summaries of each potential outcome distribution, the results are equivalent for any order of comparison and aggregation. However, for more general distributional effects, this equivalence does not hold.

²This is analogous to tree-based methods which assume the same conditional average treatment effect (CATE) for all cells assigned to a given leaf, but rather than looking for a mean shift, we measure how much of the probability density of $Y(1)$ has been “shifted” into the α -tail of $Y(0)$.

then $\beta = \alpha$ everywhere and there is no shift. Therefore, defining the alternative in this way allows us to prove desirable theoretical results both for detection power and for subset correctness, as described in Theorems 2-3 and 4-7 respectively.

As we show in Appendix A, the log-likelihood ratio statistic for (3), for a given sample, corresponds to the Berk-Jones nonparametric scan statistic [35, 10]:

$$\max_S F(S) = \max_{S, \alpha} F_\alpha^{BJ}(S) = \max_{S, \alpha} N(S) KL(\hat{\tau}_{\text{CQTE}_\alpha}(S), \alpha), \quad (4)$$

where each $\hat{\tau}_{\text{CQTE}_\alpha}(x)$ is computed using its potential outcome empirical distribution, $N(S)$ is the number of treatment group units, and $KL(\beta, \alpha) = \beta \log \frac{\beta}{\alpha} + (1 - \beta) \log \frac{1-\beta}{1-\alpha}$ is the Kullback-Leibler divergence between Bernoulli distributions with the corresponding parameters. The statistic in (4) includes a maximization over subpopulations S and thresholds α to identify the most significantly affected (highest scoring) subpopulation, and its significance can then be determined by a randomization test, appropriately controlling for multiple testing.

3 Treatment Effect Subset Scanning

Treatment Effect Subset Scan (TESS) is a novel framework for identifying subpopulations in a randomized experiment which experience treatment effects, built atop the heterogeneous quantile treatment effect test statistic established in (4). Unlike previous methods, TESS structures the challenge of treatment effect identification as an anomalous pattern detection problem—where the objective is to identify patterns of systematic deviations away from expectation—which is then solved by scanning over subpopulations. TESS therefore searches for subsets of values of each attribute for which the distributions of outcomes in the treatment groups are systematically anomalous, i.e., significantly different from their expectation as derived from the control group. More precisely, we define a real-valued outcome of interest Y and a set of discrete covariates $X = (X^1, \dots, X^d)$, where each X^j can take on a vector of values $V^j = \{v_m^j\}_{m=1 \dots |V^j|}$. We note that continuous covariates can be discretized into categories, using the observed covariate distribution or domain knowledge.³ With continuous and discrete covariates, the distribution and quantile functions are well-defined and unique for all levels $\alpha \in (0, 1)$ when the outcome Y is real-valued. We define the arity of covariate X^j as $|V^j|$ (i.e., the cardinality of V^j) and note that for any covariate profile x (i.e., a realization of X) it follows that $x \in V^1 \times \dots \times V^d$. We then define a dataset as a sample \mathcal{N} composed of n records (units) $\{R_1, \dots, R_n\}$, drawn independently and identically distributed from population \mathcal{P} . Each 3-tuple $R_i = (Y_i^{\text{obs}}, X_i, W_i)$ is described by an observed potential outcome $Y_i^{\text{obs}} = Y_i(W_i)$, covariates X_i , and an indicator variable W_i , which indicates if the unit was randomly assigned to the treatment condition; see Table 1 for a demonstrative example. We define the subpopulations S under consideration to be $S = v^1 \times \dots \times v^d$, where $v^j \subseteq V^j$. Therefore, we consider subsets S representing *subspaces* of the attribute space, i.e., the Cartesian product of a subset of values for each attribute. This is important because the treatment of interest may affect multiple values, e.g., African-Americans *or* Hispanics who live in New York *or* Pennsylvania. Finally, we

³An extension could include considering the intervals of the continuous covariate created by each of its unique split points (realized values) in the data; this is similar to how tree-based methods determine discrete splits on continuous variables.

Record	Y	X^{gender}	X^{race}	W
1	2.35	Female	Black	1
2	2.06	Female	White	1
3	2.92	Male	Black	1
4	2.27	Male	White	1
5	1.73	Female	Black	0
6	1.84	Female	White	0
7	1.7	Male	Black	0
8	1.59	Male	White	0

Table 1: This table is a demonstrative dataset of $n = 8$ records, with a $d = 2$ sized vector of covariates, $X = (X^{\text{gender}}, X^{\text{race}})$. The first, X^{gender} , can take values in $V^{\text{gender}} = \{\text{Female}, \text{Male}\}$, and the second X^{race} can take values in $V^{\text{race}} = \{\text{Black}, \text{White}\}$. A covariate profile x , and realization of X , is an element in the set of all covariate profiles $V^{\text{race}} \times V^{\text{gender}} = \{(\text{Female}, \text{Black}), (\text{Female}, \text{White}), (\text{Male}, \text{Black}), (\text{Male}, \text{White})\}$.

wish to find the most anomalous subset

$$S^* = v^{1*} \times \dots \times v^{d*} = \arg \max_S F(S), \quad (5)$$

where $F(S)$ is commonly referred to in the anomalous pattern detection literature as a score function, to measure the anomalousness of a subset S . In the context of TESS, this function is a test statistic of the treatment effect—i.e., the divergence between the treatment and control group—in subpopulation S , like the one defined in (4).

We accomplish this by first partitioning the experimental dataset into control and treatment groups, and passing the groups to the TESS algorithm. For each unique covariate profile x in the treatment group, TESS uses the control group to compute a conditional outcome distribution $\hat{\mathbb{F}}_{Y^C|X=x}$, providing an estimate of the conditional outcome distribution under the null hypothesis H_0 that the treatment has no effect on units with this profile. Then for each record R_i in the treatment group, TESS computes an empirical p -value \hat{p}_i , which serves as a measure of how uncommon it is to see an outcome as extreme as Y_i^{obs} given $X = x_i$ under H_0 . The ultimate goal of TESS is to discover subpopulations S with a large amount of evidence against H_0 , i.e., the outcomes of units in S are consistently extreme given H_0 . Thus, TESS searches for subpopulations which contain an unexpectedly large number of low (significant) empirical p -values, as such a subpopulation is more likely to have been affected by the treatment.

3.1 Estimating Reference Distributions

After partitioning the data into treatment and control groups, the TESS framework obtains an estimate of the reference distribution for each unique covariate profile in the treatment group. To obtain the estimates of $\mathbb{F}_{Y(0)|X} \forall X$, TESS relies on two assumptions: randomization and a sharp null hypothesis of no treatment effect. First, randomization implies that the potential outcomes $Y_i(0), Y_i(1) \perp\!\!\!\perp W_i \forall R_i$: selection into treatment and control groups is completely random. Secondly, the sharp null hypothesis that no subpopulation is affected by the treatment implies that $\mathbb{F}_{Y(0)|X} = \mathbb{F}_{Y(1)|X}$. With these two assumptions in hand, the TESS framework includes two options for estimating the necessary reference distributions. The first is more flexible but may encounter estimation challenges in extremely sparse, high-dimensional settings; the second is useful for higher-dimensional settings, but requires additional structural assumptions on the data generating process. Finally, given a chosen procedure for estimating reference distributions, TESS uses the distributions to

convert each observed outcome Y_i^{obs} (for data records R_i in the treatment group) to an empirical p -value range, capturing how “anomalous” that outcome is given its reference distribution.

3.1.1 Empirical Distribution Estimation

The first option we present for deriving reference distributions involves estimating the empirical conditional probability function as follows:

$$\hat{\mathbb{F}}_{Y^C|X}(y|x) = \frac{\sum_{i=1}^n \zeta_i(x) \mathbb{1}_{\{Y_i^{\text{obs}} \leq y\}}}{\sum_{i=1}^n \zeta_i(x)}, \quad (6)$$

representing a weighted average across data units, with a weight function defined as

$$\zeta_i(x) = \mathbb{1}_{\{W_i=0, X_i=x\}}. \quad (7)$$

For any record R_j in the treatment group (i.e., with $W_j = 1$) we can use $\hat{\mathbb{F}}_{Y^C|X}(\cdot|x_j)$ as an estimate of its distribution function. When we use (7) as the weight definition, then (6) amounts to the empirical density function derived from the control units that share covariate profile $X = x_j$. Moreover, it follows directly from TESS’s assumption of randomization and the Glivenko-Cantelli Theorem [22] that $\hat{\mathbb{F}}_{Y^C|X} \xrightarrow{a.s.} \mathbb{F}_{Y(0)|X}$. Therefore, TESS can use $\hat{\mathbb{F}}_{Y^C|X}$ as an unbiased and strongly-consistent estimator of the unknown $\mathbb{F}_{Y(1)|X}$ under H_0 . Intuitively, under this sharp null, the outcomes of the treatment and control groups are drawn from the same distribution, allowing $\hat{\mathbb{F}}_{Y^C|X=x}$ to serve as an outcome reference distribution for treatment units with covariate profile $X = x$.

3.1.2 Model-based Estimation

Although we define and estimate (6) individually for each unique covariate profile $X = x$ using the empirical distribution function, we note that TESS only requires some means of computing the conditional probability of observing each treatment unit outcome. The empirical distribution allows TESS to accommodate arbitrary differences in conditional outcome distributions across covariate profiles, enabling general applicability without a priori contextual knowledge. However, it is also possible to combine data across profiles to estimate the conditional probability distributions. This aggregation of information can help alleviate challenges that arise when there is data sparsity, i.e., when there are covariate profiles present in the treatment group that have few or no corresponding control data records. Intuitively, “neighboring” covariate profiles in the control group can be pooled and leveraged to improve local estimation. However, this improved estimation comes by imposing additional structure or assumptions on the underlying data generating process.

Statistical learning offers many options for distribution (or density) estimation, any of which can be utilized in TESS. We identify the Random Forest estimator that underpins the Quantile Regression Forests algorithm [36] as an attractive alternative to the purely empirical estimator described above. Random Forest can be cast as an adaptive locally weighted estimator, where the forest places more weight on observations with more similar covariates. Therefore, TESS can learn a Random Forest on the control data, still using (6) as its reference distribution, but redefining its weights as:

$$\zeta_i(x_j) = \frac{1}{B} \sum_{b=1}^B \mathbb{1}_{\{W_i=0, X_i \in L_b(x_j)\}}, \quad (8)$$

where B corresponds to the number of trees in the forest, and $L_b(x_j)$ captures the leaf node—i.e., a subset of the covariate space—of tree b that x_j falls into. Therefore, (8) can be seen as a relaxation of (7), where a control unit can have non-zero weight even if its profile does not match x_j precisely. Also the weights are adaptive and more smoothly increase with how similar a control unit is to the treatment unit. Intuitively, this adaptive similarity “kernel” is particularly helpful in sparse and/or high-dimensional settings, where the curse of dimensionality makes estimation challenging, because it allows for local estimation within covariate subspaces of similar units. Importantly, this similarity is measured along the subset of dimensions that are discovered as relevant (via the random forest learning procedure), which manifests as how often the two points would appear in the same leaf node of the learned trees. Moreover, it has been shown that such a random forest based weighting scheme for estimation can alleviate the curse of dimensionality [7]. It has also been shown that with weights as in (8), (6) is weakly-consistent, given a set of regularity conditions and the assumption that the true distribution function is Lipschitz continuous [36]. Therefore, it follows directly from this property of consistency and TESS’s assumption of randomization that $\hat{\mathbb{F}}_{Y^C|X} \xrightarrow{P} \mathbb{F}_{Y(0)|X}$. Therefore, TESS is able to use a random forest estimator of $\hat{\mathbb{F}}_{Y^C|X}$ as a weakly-consistent estimator of the unknown $\mathbb{F}_{Y(1)|X}$ under the null hypothesis H_0 .

3.2 Computing Empirical P-value Ranges

Given a mechanism for estimating the conditional probabilities of outcomes, TESS calculates an empirical p -value range [35] for each treatment unit to obtain a measure of how “anomalous” or unusual a particular unit’s outcome is given its reference distribution. For each unit R_i in the treatment group ($W_i = 1$), using (6) and an appropriate weighting scheme, the standard empirical p -value would be

$$\hat{p}(y; x) = \hat{\mathbb{F}}_{Y^C|X}(y|x) = \frac{\sum_{i=1}^n \zeta_i(x) \mathbb{1}_{\{Y_i^{\text{obs}} \leq y\}}}{\sum_{i=1}^n \zeta_i(x)}. \quad (9)$$

The empirical p -value *range* is an extension of this traditional empirical p -value, defined as

$$\begin{aligned} \hat{p}(y; x) &= [\hat{p}_{\min}(y; x), \hat{p}_{\max}(y; x)] \\ &= \left[\frac{\sum_{i=1}^n \zeta_i(x) \mathbb{1}_{\{Y_i^{\text{obs}} < y\}}}{1 + \sum_{i=1}^n \zeta_i(x)}, \frac{1 + \sum_{i=1}^n \zeta_i(x) \mathbb{1}_{\{Y_i^{\text{obs}} \leq y\}}}{1 + \sum_{i=1}^n \zeta_i(x)} \right], \end{aligned} \quad (10)$$

where the sums are taken over all control observations. The numerator of \hat{p}_{\max} , but not \hat{p}_{\min} , includes “tied” observations (i.e., $Y_i^{\text{obs}} = y$). The treatment observation y is also considered part of its own reference distribution, following from the assumption of exchangeability of control and treatment outcomes under H_0 , and thus adding one to the denominators of \hat{p}_{\min} and \hat{p}_{\max} as well as the numerator of \hat{p}_{\max} . Following [35], we use empirical p -value ranges because they improve upon traditional empirical p -values. The p -value ranges are better equipped for sparsity in high-dimensional data, as the range naturally adapts to the amount of reference data used for estimation: a treatment unit’s p -value range shrinks as more control units are used to estimate its reference distribution. Additionally, if we represented R_i with an empirical p -value \hat{p}_i that is drawn uniformly at random from its empirical p -

value range $\hat{p}(y_i; x_i)$, then under H_0 , $\hat{p}_i \sim \text{Uniform}(0, 1)$.⁴ Standard empirical p -values are only *asymptotically* distributed as $\text{Uniform}[0, 1]$ and exhibit finite sample bias, while the ranges are unbiased in finite samples, ensuring that $\mathbb{E} \left[\hat{\mathbb{F}}_{Y(1)|X=x}(\hat{\mathbb{F}}_{Y(0)|X=x}^{-1}(\alpha)) \right] = \alpha$ under H_0 .

The left-tailed p -value ranges defined in (10) identify outcomes in the extremes of the lower-tail of the reference distribution. The p -value range in relation to only the right-tail of the reference distribution or both tails can be derived from the p -value range specified for the left-tail. The right-tail range is

$$\hat{p}(y; x) = [1 - \hat{p}_{\max}(y; x), 1 - \hat{p}_{\min}(y; x)];$$

while the two-tailed range is

$$\hat{p}(y; x) = \begin{cases} [2\hat{p}_{\min}(y; x), 2\hat{p}_{\max}(y; x)] & \text{if } \hat{p}_{\max}(y; x) < 0.5 \\ [2(1 - \hat{p}_{\max}(y; x)), 2(1 - \hat{p}_{\min}(y; x))] & \text{if } \hat{p}_{\min}(y; x) \geq 0.5 \\ [2\min\{\hat{p}_{\min}(y; x), 1 - \hat{p}_{\max}(y; x)\}, 1] & \text{otherwise.} \end{cases}$$

Finally, the significance of a p -value range, for a significance level α , is defined as

$$n_\alpha(\hat{p}(y; x)) = \begin{cases} 1 & \text{if } \hat{p}_{\max}(y; x) < \alpha \\ 0 & \text{if } \hat{p}_{\min}(y; x) > \alpha \\ \frac{\alpha - \hat{p}_{\min}(y; x)}{\hat{p}_{\max}(y; x) - \hat{p}_{\min}(y; x)} & \text{otherwise.} \end{cases}$$

Intuitively, $n_\alpha(\hat{p}(y; x))$ measures the proportion of the range that is significant at level α , or equivalently, the probability that a p -value drawn uniformly from $[\hat{p}_{\min}(y; x), \hat{p}_{\max}(y; x)]$ is less than α .

3.3 Subpopulations

Given p -values as a measure of the anomalousness of individual treatment units, we now consider how TESS combines these measures to form subpopulations. For intuition, we propose representing the data as a tensor, where each covariate is represented by a mode of the tensor, $X = (X^1, \dots, X^d)$, resulting in a d -order tensor. $|V^j|$, the arity of the j^{th} covariate, is the size of the j^{th} mode. Therefore, each covariate profile x maps to a unique cell in the tensor, which contains the p -values of the treatment units that share x as their covariate profile. As stated above, a subpopulation is $S = v^1 \times \dots \times v^d$, where $v^j \subseteq V^j$; therefore, an individual cell (i.e., covariate profile x) is itself a subpopulation: $S = \{x^1\} \times \dots \times \{x^d\}$, where $x^j \in V^j$. For a demonstrative example see Table 2. For a given subpopulation S , we define the quantities

$$N_\alpha(S) = \sum_{x \in U_X(S)} \sum_{y \in Y^{Tr}(x)} n_\alpha(\hat{p}(y; x)); \quad N(S) = \sum_{x \in U_X(S)} \sum_{y \in Y^{Tr}(x)} 1 \quad (11)$$

where $U_X(S)$ is the set of non-empty covariate profiles in S , $Y^{Tr}(x) = \{Y_i^{\text{obs}} | X_i = x, W_i =$

⁴From the exchangeability under H_0 of $Y_i^{\text{obs}} \sim \mathbb{F}_{Y(1)|X}$ and $Y_j^{\text{obs}} \sim \mathbb{F}_{Y(0)|X}$, and the probability integral transform.

		Gender	
		Male	Female
Race	Black	{1.7}	{1.73}
	White	{1.59}	{1.84}

		Gender	
		Male	Female
Race	Black	{2.92}	{2.35}
	White	{2.21}	{2.06}

Control Group

Treatment Group

Table 2: A demonstrative tensor—representing the example dataset in Table 1—containing a $d = 2$ -order tensor for both the control and treatment group. The top-left cell of each tensor represents the subpopulation of black males in the data, $S = \{\text{Black}\} \times \{\text{Male}\}$. There are also the subpopulation of all males, $S = \{\text{Black}, \text{White}\} \times \{\text{Male}\}$, all black subjects, $S = \{\text{Black}\} \times \{\text{Male}, \text{Female}\}$, or the entire population, $S = \{\text{Black}, \text{White}\} \times \{\text{Male}, \text{Female}\}$; there are a total of nine subpopulations in this simple example. We note that the example dataset has only one unit with each unique covariate profile, therefore the set of values in each tensor cell is of size one.

$1\}$ is the collection of treatment units’ outcomes with covariate profile x , $N(S)$ represents the total number of empirical p -values contained in S , and $N_\alpha(S)$ is the number of p -values in S that are less than α .⁵ Given that the distribution of each p -value is $\text{Uniform}(0,1)$ under the null hypothesis that the treatment has no effect, for a subpopulation S consisting of $N(S)$ empirical p -values, $\mathbb{E}[N_\alpha(S)] = \alpha N(S)$. Under the alternative hypothesis, we expect the outcomes of the affected units to be more concentrated in the tails of their reference distributions; thus, the p -values for these affected units will be lower. Therefore, subpopulations composed of covariate profiles that are systematically affected by the treatment should express higher values of $N_\alpha(S)$ for some α . Consequently, a subpopulation S where $N_\alpha(S) > \alpha N(S)$ (i.e., with a higher than expected number of low, significant p -values) is potentially affected by the treatment.

3.4 Nonparametric Scan Statistic

TESS utilizes the nonparametric scan statistic [35, 11] to evaluate the statistical anomalousness of a subpopulation S by comparing the observed and expected number of significantly low p -values it contains. The general form of the nonparametric scan statistic is

$$F(S) = \max_{\alpha} F_{\alpha}(S) = \max_{\alpha} \Delta(\alpha, N_{\alpha}(S), N(S)),$$

where $N_{\alpha}(S)$ and $N(S)$ are defined as in (11), and Δ is a measure of divergence measuring the anomalousness of the p -values in S . See Appendix A for a collection of goodness-of-fit scoring functions written in the general form of the nonparametric scan statistic. As described in (4), in this work we utilize the Berk-Jones scan statistic: $\max_{\alpha} \Delta_{BJ}(\alpha, N_{\alpha}(S), N(S)) = \max_{\alpha} N(S) KL\left(\frac{N_{\alpha}(S)}{N(S)}, \alpha\right)$, a log-likelihood ratio test statistic of the distributional treatment effect in subpopulation S . Maximizing $F(S)$ over a range of α , rather than a single arbitrarily-chosen α value, enables TESS to detect a small number of highly anomalous p -values, a larger subpopulation with subtly anomalous p -values, or anything in between. We consider “significance levels” $\alpha \in [\alpha_{\min}, \alpha_{\max}]$, for constants $0 < \alpha_{\min} < \alpha_{\max} < 1$. The range of α to consider can be specified based on the quantile values of interest. The choice of α_{\max} describes how extreme a value must be, as compared to the reference distribution, in order to be considered significant. We often choose $\alpha_{\min} \approx 0$, but larger values can be used to avoid returning subsets with a small number of extremely significant p -values.

⁵For p -value ranges, as in [35], $N_{\alpha}(S)$ is more precisely the total probability mass less than α over the p -value ranges in S .

3.4.1 Efficient Scanning

The next step in the TESS framework is to detect the subpopulation most affected by the treatment, i.e., to identify the most anomalous subset of values for each of the d modes of the tensor, or equivalently for each covariate $X^1 \dots X^d$. More specifically, the goal is to identify the set of subsets $\{v^1, \dots, v^d\}$ where each element corresponds to values in a tensor-mode (covariate), such that $F(v^1 \times \dots \times v^d)$ is jointly maximized. The computational complexity of solving this optimization naively is $O(2^{\sum_j |V^j|})$, where $|V^j|$ is the size of mode j (the arity of X^j), and is computationally infeasible for even moderately sized datasets.

We therefore employ the linear-time subset scanning property (LTSS) [38], which allows for efficient and exact maximization of any function satisfying LTSS over all subsets of the data. We formally define the LTSS property below, but intuitively it guarantees that the optimization over all subsets S can be done by ranking data elements (according to a specific “priority function”) and then only considering the top- t subsets as candidates.

LTSS Property Definition: Given a set of data elements $R = \{R_1, \dots, R_n\}$, a score function $F(S)$ mapping $S \subseteq R$ to a real number, and a priority function $G(R_i)$ mapping a single data element $R_i \in R$ to a real number. If $F(S)$ satisfies the *LTSS property* with priority function $G(R_i)$, then the only subsets with the potential to be optimal are those consisting of the top- t highest priority records, $S \in \{\{R_{(1)}, \dots, R_{(t)}\}\}_{t \in \{1, 2, \dots, n\}}$. In other words, there exists some $t \in \{1, 2, \dots, n\}$ such that $\arg \max_S F(S) = \{R_{(1)}, \dots, R_{(t)}\}$. We also formally restate the original LTSS theorem:

Theorem 1 ([38]). *Let $F(S) = F(X, Y)$ be a function of two additive sufficient statistics of subset S , $X(S) = \sum_{R_i \in S} x_i$ and $Y(S) = \sum_{R_i \in S} y_i$, where x_i and y_i depend only on element R_i . Assume that $F(S)$ is monotonically increasing with $X(S)$, that all y_i values are positive, and that $F(X, Y)$ is convex. Then $F(S)$ satisfies the LTSS property with priority function $G(R_i) = \frac{x_i}{y_i}$.*

In this work, we use Theorem 1 to optimize $F_\alpha(S) = \Delta(\alpha, N_\alpha(S), N(S))$ with a fixed value of α ; therefore, $X(S) = N_\alpha(S)$ and $Y(S) = N(S)$ are “additive sufficient statistics”, i.e., both $N_\alpha(S)$ and $N(S)$ are additive statistics of S , from (11), and $F_\alpha(S)$ can be written as $F_\alpha(N_\alpha(S), N(S))$. Moreover, for $F_\alpha(S)$ (with α fixed) to satisfy LTSS, we also assume: (A1) Δ is monotonically **increasing** w.r.t. N_α , (A2) Δ is monotonically **decreasing** w.r.t. N , and (A3) Δ is **convex** w.r.t. N_α and N . These properties are intuitive because the ratio of observed to expected number of significant p -values $\frac{N_\alpha}{\alpha N}$ increases with the numerator (A1) and decreases with the denominator (A2). Also, a fixed ratio of observed to expected is more significant when the observed and expected counts are large (A3). In Appendix A, we show that nonparametric scan statistics using a large class of goodness of fit functions, including the Berk-Jones scan statistic utilized in this work, exhibit these properties.

We now extend Theorem 1 to the (potentially high-dimensional) tensor context using Corollary 1 below. Essentially, the corollary demonstrates that the nonparametric scan statistic satisfies LTSS in the context of TESS, and therefore a single mode of a tensor can be efficiently optimized over subsets, conditioned on the subsets of values for the other modes. Let $U_\alpha(S)$ be the set of unique p -values between α_{\min} and α_{\max} contained in subpopulation S . Then the quantity $\max_S F(S) = \max_{\alpha \in U_\alpha(S)} \max_S F_\alpha(S)$ can be efficiently and exactly computed over all subsets $S = v^j \times v^{-j}$, where $v^j \subseteq V^j$, for a given subset of values for each

of the other modes v^{-j} .⁶ To do so, consider the set of distinct α values, $U = U_\alpha(V^j \times v^{-j})$. For each $\alpha \in U$ we employ the logic described in Corollary (1) to optimize $F_\alpha(S)$: we compute the priority $G_\alpha(v_m^j)$ for each value ($v_m^j \in V^j$), sort the values based on priority function $G_\alpha(v_m^j)$, and evaluate subsets of the form $S = \{v_{(1)}^j, \dots, v_{(t)}^j\} \times v^{-j}$ consisting of the top- t highest priority values, for $t = 1, \dots, |V^j|$.

Corollary 1. *Consider the nonparametric scan statistics $F(S) = \max_\alpha F_\alpha(S)$, where the significance level $\alpha \in [\alpha_{\min}, \alpha_{\max}]$, for constants $0 < \alpha_{\min} < \alpha_{\max} < 1$. For a given value of α and $v^{-j} = v^1 \times \dots \times v^{j-1} \times v^{j+1} \times \dots \times v^d$ under consideration, $F_\alpha(S)$ can be efficiently maximized over all subpopulations $S = v^j \times v^{-j}$, for $v^j \subseteq V^j$.*

Proof. We have $F_\alpha(S) = \Delta(\alpha, N_\alpha(v^j), N(v^j))$, with the additive sufficient statistics $N_\alpha(v^j) = \sum_{x \in U_X(v^j \times v^{-j})} \sum_{y \in Y^{Tr}(x)} n_\alpha(\hat{p}(y; x))$ and $N(v^j) = \sum_{x \in U_X(v^j \times v^{-j})} \sum_{y \in Y^{Tr}(x)} 1$, noting that the number of p -values in every v^j is positive, as we only consider the values of a covariate that are expressed by some treatment unit. Since the nonparametric scan statistic is defined to be monotonically increasing with N_α (A1), monotonically decreasing with N (A2), and convex (A3), we know that $F_\alpha(S)$ satisfies the LTSS property with priority function, over the values of mode (covariate) j , $G_\alpha(v_m^j) = \frac{\sum_{x \in U_X(v_m^j \times v^{-j})} \sum_{y \in Y^{Tr}(x)} n_\alpha(\hat{p}(y; x))}{\sum_{x \in U_X(v_m^j \times v^{-j})} \sum_{y \in Y^{Tr}(x)} 1}$ for $v_m^j \in V^j$. Therefore the LTSS property holds for each value of α , enabling each $F_\alpha(S)$ to be efficiently maximized over subsets of values for the j^{th} mode of the tensor, given values for the other $d - 1$ modes. \square

TESS iterates over modes of the tensor, using the efficient optimization steps described above to optimize each mode: $v^j = \arg \max_{v^j \subseteq V^j} F(v^j \times v^{-j})$, $j = 1 \dots d$. The cycle of optimizing each mode continues until convergence, at which point TESS has reached a conditional maximum of the score function, i.e., v^j is conditionally optimal given v^{-j} for all $j = 1 \dots d$. This ordinal ascent approach is not guaranteed to converge to the joint optimum, but with multiple random restarts the combination of subset scanning and ordinal ascent has been shown to locate near globally optimal subsets with high probability [39, 35]. We further provide asymptotic guarantees for TESS to recover the precisely correct subpopulation that is also shown to be the globally optimal subset (Theorems 6 and 7). Moreover, if $\sum_{j=1}^d |V^j|$ is large, this iterative procedure makes the ability to detect anomalous subpopulations computationally feasible, without excluding potentially optimal subpopulations from the search space (as a greedy top-down approach may). A single iteration (optimization of mode j of the tensor) has a complexity of $O(|U| (n_t + |V^j| \log |V^j|))$, where the n_t term—the number of treatment units—results from collecting the p -values for all units in $V^j \times v^{-j}$ over our sparse tensor; $U = U_\alpha(V^j \times v^{-j})$, with $|U| \leq n_t$ [35]; and $O(|V^j| \log |V^j|)$ is required to sort, based on the priority, the values of tensor mode j . Therefore a step in the procedure (a sequence of d iterations over all modes of the tensor) has complexity $O(\bar{U}d(n_t + \bar{V} \log \bar{V}))$, where \bar{U} and \bar{V} are the average numbers of α thresholds considered and covariate arity, respectively. Thus the TESS search procedure has a total complexity of $O(I\bar{Z}\bar{U}d(n_t + \bar{V} \log \bar{V}))$, where I is the number of random restarts and \bar{Z} is the average number of iterations required for convergence. We note that \bar{Z} is typically very small; $\bar{Z} \leq 5$ across all simulations discussed in §5.

⁶Note that for convenience of notation we define $S = v^j \times v^{-j}$; however, the elements of the set v^j still appear at the j^{th} position of the covariate profiles in S .

3.5 TESS Algorithm

Inputs: randomized experiment dataset, α_{\min} , α_{\max} , number of iterations I .

1. For each unique covariate profile x in the treatment group:
 - (a) Estimate $\hat{\mathbb{F}}_{Y^C|X=x}$ from the outcomes of the units in the control group.
 - (b) Compute the p -value (range) $\hat{p}_i = \hat{p}(y_i; x_i)$ for each treatment unit i with profile x from $\hat{\mathbb{F}}_{Y^C|X=x}$.
2. Iterate the following steps I times. Record the maximum value \hat{F}^* of $F(S)$, and the corresponding subset of values v^{j*} for each of the d modes, over all such iterations:
 - (a) For each of the d modes, initialize v^j to a random subset of values V^j .
 - (b) Repeat until convergence:
 - i. For each of the d modes:
 - A. Maximize $F(S) = \max_{\alpha \in [\alpha_{\min}, \alpha_{\max}]} F_\alpha(v^j \times v^{-j})$ over subsets of values for j^{th} mode $v^j \subseteq V^j$, for the current subset of values of the other $d-1$ modes v^{-j} , and set $v^j \leftarrow \arg \max_{v^j \subseteq V^j} F(v^j \times v^{-j})$.
3. Output $\hat{S}^* = v^{1*} \times \dots \times v^{d*}$ and the corresponding score $\hat{F}^* = F(\hat{S}^*)$.

3.6 Estimator Properties

In the above sections we outline a procedure to efficiently estimate $\max_{S \in Rect} F(S)$, where $Rect$ represents the space of all rectangular subsets of D . In this section we treat $\max_{S \in Rect} F(S)$ as a statistic of the data, and aim to show that it has desirable statistical properties. It is known that for data $X_1, \dots, X_n \stackrel{iid}{\sim} \mathbb{F}$ and the corresponding empirical distribution function \mathbb{F}_n , $\|\mathbb{F}_n - \mathbb{F}\|_\infty \xrightarrow{a.s.} 0$. Many goodness-of-fit statistics $GoF(\mathbb{F}_n, \mathbb{F})$ are equivalent to an empirical process over centered and scaled empirical measures; and empirical process theory provides tools to control Type I and II error [22, 17, 44]. However, in a general sense our goal is to control the behavior of $\max_{S \subseteq \{X_1, \dots, X_n\}} GoF(\mathbb{F}_S, \mathbb{F})$, where \mathbb{F}_S is the empirical distribution given by the subset S . It is not obvious whether the desirable properties present for \mathbb{F}_n will persist when considering the empirical distribution of \mathbb{F}_S , a non-random subset of the data chosen by our optimization procedure. Given that this context of optimization over subsets is not considered in the current goodness-of-fit literature, we provide various theoretical results in support of our subset scanning algorithm. In the remainder of the section we present the key statements necessary to show our desired properties below, while additional results and all proofs can be found in Appendix B. We begin with the fact that our score function can be considered a test statistic for a hypothesis test analogous to that described in (3):

$$\begin{aligned}
 H_0 : Y_i(1)|X_i &\sim \mathbb{F}_{Y_i(0)|X_i} \quad \forall X_i \in U_X(D) \\
 H_1(S) : \begin{cases} Y_i(1)|X_i &\not\sim \mathbb{F}_{Y_i(0)|X_i} \quad \forall X_i \in U_X(S), S \in Rect \\ Y_i(1)|X_i &\sim \mathbb{F}_{Y_i(0)|X_i} \quad \forall X_i \notin U_X(S), S \in Rect \end{cases}
 \end{aligned} \tag{12}$$

where D is our dataset (or tensor) of treatment units and $Rect$ is the set of all rectangular subsets of D .⁷ The null hypothesis is that all of the observed outcomes of treatment units are drawn from the same conditional outcome distribution (given the observed covariates) as their control group. Recall that $U_X(D)$ is the set of unique covariate profiles (non-empty tensor cells) in our data, with cardinality $|U_X(D)| = M$; while $S^* = \arg \max_{S \in Rect} F(S)$ and $S_u^* = \arg \max_S F(S)$ represent the most anomalous rectangularly constrained subset and the most anomalous unconstrained subset respectively. For mathematical convenience, we assume $N(x) = n$ for all $x \in U_X(D)$, i.e., n units belong to each unique covariate profile (non-empty cell) in the data and treatment condition.⁸ We consider the case where $n \rightarrow \infty$, maximizing $F(S) = \max_{\alpha \in [\alpha_{\min}, \alpha_{\max}]} F_\alpha(S)$ for $0 < \alpha_{\min} < \alpha_{\max} < 1$. We can therefore demonstrate:

Lemma 1. *Under H_0 defined in (12), let $N(x) = n \forall x \in U_X(D)$, then as $n \rightarrow \infty$,*

$$\begin{aligned} \sqrt{F(S_u^*)} &\xrightarrow{d} G(\mathbb{W}(\alpha_{\min}, \alpha_{\max}), M) \\ &\leq C\sqrt{M} + \frac{\mathbb{W}(\alpha_{\min}, \alpha_{\max})}{\sqrt{2}}, \end{aligned}$$

where the function G and constant $C < 1$ are known; $\mathbb{W}(\alpha_{\min}, \alpha_{\max}) = \sup_{\alpha \in [\alpha_{\min}, \alpha_{\max}]} \frac{|B(\alpha)|}{\sqrt{\alpha(1-\alpha)}}$, and $B(\alpha)$ represents a Brownian bridge on $[0, 1]$.

Thus, when the null hypothesis is true, the most anomalous unconstrained subset's score distribution can be upper bounded. Our ability to understand the limiting behavior of the $F(S_u^*)$ exploits its structure, which we get from LTSS theory: the optimal unconstrained subset will be $S_u^* \in \{\{x_{(1)}, \dots, x_{(t)}\}\}_{t \in \{1, 2, \dots, M\}}$, where $x_{(t)}$ has the t^{th} largest value of the random variable $\frac{N_\alpha(x)}{N(x)} \forall x \in U_X(D)$. Next we note that the score maximized over the space of unconstrained subsets upper bounds the score maximized over the subspace of rectangular subsets, i.e., $F(S^*) \leq F(S_u^*)$. We use this fact to obtain the following result:

Theorem 2. *Under H_0 defined in (12), let $N(x) = n \forall x \in U_X(D)$ and fix Type-I error rate $\delta > 0$, then there exists a critical value $h(\delta)$ such that*

$$\lim_{n \rightarrow \infty} P_{H_0} \left(\max_{S \in Rect} F(S) > h(\delta) \right) \leq \delta.$$

Theorem 2 indicates that $\max_{S \in Rect} F(S)$ provides a statistic to quantify the evidence to reject H_0 , enabling an (asymptotically) valid δ -level hypothesis test such that $P_{H_0}(\text{Reject } H_0) \leq \delta$, for any fixed Type I error rate $\delta > 0$. From the proof of Theorem 2, in Appendix B, we derive that $h(\delta) = \left(0.45\sqrt{M} + \frac{w(\delta)}{\sqrt{2}}\right)^2$, where $w(\delta)$ returns w such that $P(\mathbb{W}(\alpha_{\min}, \alpha_{\max}) > w) = \delta$. For intuition, $w(\delta)$ is typically small, e.g., $w(\delta) \approx 5.81$ for $\delta = 10^{-6}$ and $(\alpha_{\min}, \alpha_{\max}) = (.01, .99)$. We note that because we are maximizing both over subsets S and thresholds α , these results are distinct from the straightforward application of known results

⁷The null hypotheses defined in (3) and (12) are analogous because if $\tau_{\text{CQTE}_\alpha}(x) = \alpha \forall x \in S, \forall \alpha$, then the distributions for $Y(1)|X$ and $Y(0)|X$ are the same. Similarly, the alternative hypotheses are analogous because if $\exists \beta > \alpha$ such that $\tau_{\text{CQTE}_\alpha}(x) = \beta \forall x \in S$, then $Y(1)|X$ is different from $Y(0)|X$, and if $\tau_{\text{CQTE}_\alpha}(x) = \alpha \forall x \notin S, \forall \alpha$, then again the distributions for $Y(1)|X$ and $Y(0)|X$ are the same.

⁸We can redefine $n = \min_x N(x) \forall x \in U_X(D)$ and our results can be extended.

from empirical process theory or Dvoretzky-Kiefer-Wolfowitz bounds, which would give us $\max_{\alpha} \left| \frac{N_{\alpha}(S)}{N(S)} - \alpha \right| \rightarrow 0$ for a given S .

Next, we turn our attention to the alternative hypothesis, where $S^T \in \text{Rect}$ represents the truly affected subset, $k = \frac{|U_X(S^T)|}{|U_X(D)|}$ is the proportion of covariate profiles included in S^T , and $H_1(S^T)$ implies that there exist constants α and $\beta(\alpha) > \alpha$ such that $\beta(\alpha) = \mathbb{F}_{Y(1)|X=x}(\mathbb{F}_{Y(0)|X=x}^{-1}(\alpha))$ for all $x \in U_X(S^T)$. We then have the following results:

Lemma 2. *Under $H_1(S^T)$ defined in (12), let $N(x) = n \forall x \in U_X(D)$, and consider $F_{\alpha^*}(S^T)$ for $\alpha^* = \arg \max_{\alpha \in [\alpha_{\min}, \alpha_{\max}]} \frac{(\beta(\alpha) - \alpha)^2}{2\alpha(1-\alpha)}$ and $\beta^* = \beta(\alpha^*)$. Then as $n \rightarrow \infty$,*

$$\sqrt{F_{\alpha^*}(S^T)} - O\left(\sqrt{kMn}\right) \xrightarrow{d} \text{Gaussian}(0, \sigma_{\alpha^*\beta^*}^2),$$

where $\sigma_{\alpha^*\beta^*}^2 > 0$ does not depend on k , M , or n .

Thus, when the null hypothesis is false, the expected value of the true subset's score at the α^* quantile, $F_{\alpha^*}(S^T)$, is increasing with n . This result, and the fact that $F_{\alpha}(S) \leq F(S) \forall S, \alpha$, are used to obtain the following result:

Theorem 3. *Under $H_1(S^T)$ defined in (12), let $N(x) = n \forall x \in U_X(D)$ and critical value $h(\delta)$ be set for the same fixed Type-I error rate $\delta > 0$ as in Theorem 2, then*

$$\lim_{n \rightarrow \infty} P_{H_1} \left(\max_{S \in \text{Rect}} F(S) > h(\delta) \right) = 1.$$

As a consequence of Theorem 3, the δ -level hypothesis test based on $\max_{S \in \text{Rect}} F(S)$ has full asymptotic power $P_{H_1}(\text{Reject } H_0) \rightarrow 1$. Note that in this context we consider a fixed alternative $\beta(\alpha)$, as opposed to a local alternative where $\beta_n(\alpha) \rightarrow \alpha$ as $n \rightarrow \infty$.

In practice, when we consider an experiment with finite M and n , permutation testing can be used to control the Type I error rate of our scanning procedure, and conditions have been shown where permutation calibrations achieve the Type II error rates of an oracle scan test [4]. These theoretical and practical results intuitively capture our statistic's ability to conclude that the null hypothesis is false—i.e., that there exists some subset that follows H_1 , and therefore invalidates H_0 . However, this does not necessarily provide a guarantee that the statistic will exactly capture the true subset. Therefore, next we derive finite sample sufficient conditions under which our framework achieves subset correctness: $S^* = S^T$. We then show asymptotic convergence of $P(S^* = S^T) \rightarrow 1$ as $n \rightarrow \infty$.

We introduce additional notation for this discussion: $r_{\text{mle}}(x) = \frac{N_{\alpha}(x)}{N(x)} - \alpha$, $r_{\text{mle}-h}^{\text{aff}} = \max_{x \in U_X(S^T)} r_{\text{mle}}(x)$, $r_{\text{mle}-l}^{\text{aff}} = \min_{x \in U_X(S^T)} r_{\text{mle}}(x)$, $r_{\text{mle}-h}^{\text{unaff}} = \max_{x \notin U_X(S^T)} r_{\text{mle}}(x)$, and $\eta = \left(\frac{\sum_{x \in U_X(S^T)} N(x)}{\sum_{x \in U_X(D)} N(x)} \right)$. We also introduce the concepts of ν -homogeneous, which means that $\frac{r_{\text{mle}-h}^{\text{aff}}}{r_{\text{mle}-l}^{\text{aff}}} < \nu$, and δ -strong, which means that $\frac{r_{\text{mle}-l}^{\text{aff}}}{r_{\text{mle}-h}^{\text{unaff}}} > \delta$. Intuitively, the concept of *homogeneity* measures how similarly the treatment affects each $\mathbb{F}_{Y|X=x}$ for $x \in U_X(S^T)$, while *strength* measures how large of an effect the treatment exhibits across all $\mathbb{F}_{Y|X=x}$ for $x \in U_X(S^T)$. More specifically, these concepts respectively imply that for any pair of the affected covariate profiles $(x_i, x_j \in U_X(S^T))$, the anomalous signal (i.e., treatment effect) observed in x_i is less than ν times that which is observed in x_j , and the treatment effect observed in every affected covariate profile is more than δ times that of the unaffected profiles. Using these concepts we have the following results:

Theorem 4. Under $H_1(S^T)$ defined in (12), where $|U_X(S^T)| = t > 0$, $\exists \nu > 1$ such that if the observed effect across the t covariate profiles in S^T is ν -homogeneous, and at least 1-strong, then the highest scoring subset $S^* \supseteq S^T$.

Theorem 5. Under $H_1(S^T)$ defined in (12), where $|U_X(S^T)| = t > 0$, $\exists \delta > 1$ such that if the observed effect across the t covariate profiles in S^T is $\frac{\delta}{\eta}$ -strong, then the highest scoring subset $S^* \subseteq S^T$.

Theorem 6. Under $H_1(S^T)$ defined in, where $|U_X(S^T)| = t > 0$, let $N(x) = n \forall x \in U_X(D)$. If $|U_X(D)| = M$ is fixed then as $n \rightarrow \infty$, $P(S^* = S^T) \rightarrow 1$.

While Theorem 6 shows that $S^* = S^T$ with high probability as $n \rightarrow \infty$ —i.e., the most anomalous (rectangular) subset is the true subset—it does not guarantee that the TESS algorithm presented in Section 3.5 will converge to the true subset, because iterative ascent algorithms converge to a local maximum. For example, if Step 2(a) of the algorithm chooses an initial subset S_0 that is disjoint from S^T , then it is possible that no maximization over subsets of values for any single mode in Step 2(b).i.A. will improve the score, and TESS will fail to identify S^T on that iteration. However, we can show the following:

Theorem 7. Under $H_1(S^T)$ defined in (12), where $|U_X(S^T)| = t > 0$ and $S^T \in \text{Rect}$, let $N(x) = n \forall x \in U_X(D)$. Assume $|U_X(D)| = M$ is fixed. Let \hat{S}^* denote the subset returned by a given iteration of the TESS algorithm, which was initialized to some subset $S_0 \in \text{Rect}$, such that $S^T \cap S_0 \neq \emptyset$. Then as $n \rightarrow \infty$, $P(\hat{S}^* = S^T) \rightarrow 1$.

Thus as $n \rightarrow \infty$ for fixed M , TESS will identify the correct rectangular subset S^T w.h.p., as long as it is initialized to some rectangular subset S_0 that overlaps S^T , for at least one of its iterations. For example, S_0 could be the entire dataset D , thus guaranteeing $S_0 \cap S^T \neq \emptyset$.

Together, these results demonstrate that the test statistic $F^* = \max_{S \in \text{Rect}} F(S)$ and corresponding subset $S^* = \arg \max_{S \in \text{Rect}} F(S)$ possess desirable statistical properties. Theorems 2 and 3 imply that the asymptotic Type I and II errors of our procedure can be controlled, with implications for maximization over subsets of empirical processes more generally. Theorems 4 and 5 indicate that for a score function there exist constants ν and δ that define how similar and strong the treatment effect must be in the affected subpopulation, to ensure that the highest-scoring subset corresponds exactly to the true affected subset $S^* = S^T$. Finally, Theorem 6 shows asymptotic convergence for $P(S^* = S^T) \rightarrow 1$ as $n \rightarrow \infty$, and Theorem 7 shows that the TESS algorithm will identify S^T w.h.p. as $n \rightarrow \infty$. To our knowledge, this is the first work on heterogeneous treatment effects that provides conditions on the exactness of subpopulation discovery.

4 Related Work

There has been a growing literature using statistical learning methods to provide data-driven approaches for estimating heterogeneous treatment effects in randomized experiments. Recent work has adapted regularized regression for treatment effect heterogeneity [26, 47, 52]. These regularized regression approaches, however, require the researcher to select which covariate and treatment interactions to include in the model specification, compromising their ability to *discover* unexpected treatment patterns in subpopulations.

Regression tree based methods [46, 6] select subpopulations and estimate treatment effects by recursively partitioning the data into homogeneous subpopulations that share a subset of covariate profile values and have similar outcomes. The effectiveness of tree methods can be severely compromised in many settings as a result of their greedy partitioning.⁹ Tree models can be unstable; they can provide extremely discontinuous approximations of an underlying smooth function, limiting overall accuracy; and they can struggle to estimate functions which exhibit specific properties, including when a small proportion of the covariates constitute the influential interactions [21].

Other treatment effect estimation approaches use ensemble methods, including the use of Bayesian Additive Regression Trees [25, 23], Random Forests [20, 51], and ensembles of strong learners [24]. Ensembles provide more stable and smooth function estimates [51]; however, they lose the interpretability of natural groupings (e.g., specific combinations of covariates or clearly defined leaves) which is important for *identifying* affected subpopulations.

Finally, [12] propose approaches to test if there is detectable heterogeneity in treatment effects, finding the quantiles exhibiting heterogeneous treatment effects induced by the machine learning proxy predictors, and then identifying the covariates that appear associated with the heterogeneity. Therefore this approach is a post-hoc analysis of existing machine learning predictors (e.g., regression tree or ensemble methods) which are optimized for overall risk minimization and not the discovery of subpopulations with significant treatment effects. Furthermore, there are orthogonal research streams focused on (heterogeneous) treatment assignment that include policy learning [54, 8] and welfare maximization [29, 34] in observational and experimental data. These methods assign a personalized treatment for each individual unit. Instead, TESS takes as input a set of units which have already been randomly assigned a treatment.

Although this literature contains a growing set of novel statistical learning methods for causal inference, at the core of the majority of these approaches are objective functions designed for flexible estimation (and risk minimization) instead of subpopulation discovery (and significant effect maximization). TESS is therefore unique as it is optimized to discover interpretable subpopulations that exhibit significant evidence of treatment effects. When necessary, TESS can use flexible (risk minimizing) statistical learning models for a purpose that is aligned with their objective: as an accurate estimator of the conditional outcome distribution for the control group as in Section 3.1.2.

5 Empirical Analysis

In this section we empirically demonstrate the utility of the TESS framework as a tool to identify subpopulations with significant treatment effects. We use data from the Tennessee Student/Teacher Achievement Ratio (STAR) randomized experiment [53] in order to provide representative performance in real-world policy analysis. We review the original STAR data (§5.1), and describe our procedure for simulating affected subpopulations (§5.2).

Through the simulation results described in §5.3, we compare the ability of TESS to detect significant subpopulations to three recently proposed statistical learning approaches: Causal Tree [6], Interaction Tree [46, 6], and Causal Forest [51]. Specifically, we evaluate

⁹Though there are non-greedy tree based learning methods, these methods are used for optimal treatment assignments for individual units in observational data [54].

each method on two general metrics: detection power and subpopulation accuracy. Detection power measures $P_{H_1}(\text{Reject } H_0)$, or how well a method can detect the existence—not necessarily the location—of treatment effect heterogeneity in the experiment. Subpopulation accuracy, on the other hand, is specifically designed to measure how well a method can precisely and completely capture the subpopulation(s) with significant treatment effects.

Finally, we conduct an exploratory analysis of the STAR dataset, and in §5.4 discuss the subpopulations identified by TESS as affected by treatments. In some cases, the identified subpopulation is consistent with the literature on the STAR experiment; in other cases, TESS uncovers previously unreported, but intuitive and believable, subpopulations. These empirical results demonstrate TESS’s potential to generate potentially useful and non-obvious hypotheses for further exploration and testing.

5.1 Tennessee STAR Experiment

The Tennessee Student/Teacher Achievement Ratio (STAR) experiment is a large-scale, four-year, longitudinal randomized experiment started in 1985 by the Tennessee legislature to measure the effect of class size on student educational outcomes, as measured by standardized test scores. The experiment started monitoring students in kindergarten (during the 1985-1986 school year) and followed students until third grade. Students and teachers were randomly assigned into conditions during the first school year, with the intention for students to continue in their class-size condition for the entirety of the experiment. The three potential experiment conditions were not based solely on class size, but also the presence of a full-time teaching aide: small classrooms (13-17 pupils), regular-size classrooms (22-25 pupils), and regular-size classrooms with aide (still 22-25 pupils). Therefore, the difference between the former two conditions is classroom size, and the difference between the latter two conditions is the inclusion of a full-time teacher’s aide in the classroom. The experiment included approximately 350 classrooms from 80 schools, each of which had at least one classroom of each type. Each year more than 6,000 students participated in this experiment, with the final sample including approximately 11,600 unique students.

The Tennessee STAR dataset has been well studied and analyzed, both by the project’s internal research team [53, 19] and by external researchers [33, 40]. As indicated by [33], the investigations have primarily focused on comparing means and computing average treatment effects. [33] presents a detailed econometric analysis and draws similar conclusions to the previous research: students in small classrooms perform better than those in regular classrooms, while there is no significant effect of a full-time teacher’s aide, or moderation from teacher characteristics. Moreover, the effect accumulates each year a student spends in a small classroom [33]. Additionally, these conclusions are robust in the presence of potentially compromising experimental design challenges: imbalanced attrition, subsequent changes in original treatment assignment, and fluctuating class sizes [33].

5.2 Experimental Simulation Setup

The goal of our experimental simulation is to replicate conditions under which a researcher would want to use an algorithm to discover subpopulations with significant treatment effects, and to observe how capable various algorithms are at identifying the correct subpopulation(s). In order to replicate realistic conditions, we use the STAR experiment as our base dataset, and inject into it subpopulations (of a given size) with a treatment effect

(of a given magnitude). More specifically, we treat each student-year as a unique record and for each record capture ten covariates: student gender, student ethnicity, grade, STAR treatment condition, free-lunch indicator, school development environment, teacher degree, teacher ladder, teacher experience, and teacher ethnicity. We note that each of these variables, other than teacher experience, is discrete; we discretize experience into five-year intervals: $[0, 5)$, $[5, 10)$, \dots , $[30, \infty)$. The number of values a covariate can take ranges from two to eight. By preserving the overall data structure of the STAR experiment—number of covariates, covariate value correlations, subpopulations, sample sizes, etc.—our simulations are more able to replicate the structure (and challenges) faced by experimenters.

The process we follow to generate a simulated treatment effect begins with selecting a subpopulation S_{affected} to affect. Recall that the dataset contains a set of discrete covariates $X = (X^1, \dots, X^d)$, where each X^j can take on a vector of values $V^j = \{v_m^j\}_{m=1 \dots |V^j|}$ and $|V^j|$ is the arity of covariate X^j . Therefore, we define a subpopulation as $S = v^1 \times \dots \times v^d$, where $v^j \subseteq V^j$. The affected subpopulation is generated at random based on two parameters: *num_covs*, or the number of covariates to select, and *value_prob*, or probability a covariate value is selected. We select *num_covs* covariates at random, and for each of these covariates we select each of their values with probability equal to *value_prob*, ensuring that at least one value for each of these covariates is selected. The final affected subpopulation is then $S_{\text{affected}} = v^1 \times \dots \times v^d$, where v^j is the selected values if X^j is one of the *num_covs* covariates, and otherwise $v^j = V^j$. In other words, for a random subset of covariates, S_{affected} only includes a random subset of their values, and for all other covariates S_{affected} includes all of their values. This treatment effect simulation scheme allows for variation in the size of the subpopulation that is affected: instances of S_{affected} can constitute a small subpopulation (a challenging detection task), a large subpopulation (a relatively easier detection task), or something in between. Therefore a set of simulations, with varying parameter values, captures the spectrum of conditions a researcher may face when analyzing an experiment to identify subpopulations with significant treatment effects.

The next step in the process involves partitioning the dataset into treatment and control groups, and generating outcomes for each record. Outcomes are drawn randomly from one of two distributions: the null distribution (f_0) or the alternative distribution (f_1). Any record in the treatment group that has a covariate profile $x \in U_X(S_{\text{affected}})$ has outcomes generated by f_1 ; all other records have outcomes drawn from f_0 . Therefore only S_{affected} has a treatment effect, whose effect magnitude is the distributional difference between f_0 and f_1 , represented by the parameter δ .

Each of the methods we consider in these experiments has a unique approach to identifying potential subpopulations with differential treatment effects. Furthermore, as mentioned in §4, most methods in the literature do not provide a process for identifying extreme treatment effects. Therefore, we devise intuitive post-processing steps in an attempt to represent how researchers would use each method to identify potential subpopulations that have significant treatment effects. Each method returns identified subpopulations and corresponding scores (measures) of the treatment effect. For the single tree-based methods [6, 46] we follow the suggestion of [6] to perform inference (via a two-sample Welch T-Test) in each leaf of the tree, and we then sort the leaves based on their statistical significance. The final subpopulation returned by the tree is the leaf with the most statistically significant treatment effect, and the final treatment effect measure is this leaf’s statistical significance (*p*-value). For a method that provides an individual level treatment effect (and estimate of

variance) [51], we propose to perform inference for each unique covariate profile, and return those that are statistically significant. The final treatment effect measure is the smallest p -value of the covariate profiles. We empirically compare these prominent methods from the literature to our TESS algorithm, selecting the Berk-Jones nonparametric scan statistic to score a subset (§2) and the most general empirical estimation approach to model the reference distribution (§3.1.1). The TESS algorithm, by design, provides the subpopulation it determines to have a statistically significant distributional change (treatment effect) and a measure of this change, so no post-processing is necessary.

5.2.1 Detection Power

For any given combination of simulation parameter values $(\delta, num_covs, value_prob)$, detection power measures $P(Reject\ H_0 \mid H_1(S_{affected}))$, or how well a method is able to identify the presence of $S_{affected}$. This is accomplished by comparing the treatment effect measure (score of the detected subset) found under $H_1(S_{affected})$ to the distribution of the treatment effect measure under H_0 . More specifically, for a given set of parameter values, we generate a random dataset which only exhibits a treatment effect in the randomly selected subpopulation $S_{affected}$; each method attempts to detect this subpopulation. As described in §5.2, each method returns a final treatment effect measure for the subpopulation it detects in this affected dataset. For the same dataset, we then conduct randomization testing to determine how significant this treatment effect measure is under H_0 . We make many copies of the dataset (1000 in our experiments) and in each copy, we generate new outcomes (drawn from f_0) such that no subpopulation has a treatment effect. Each method then generates a detected subpopulation and corresponding treatment effect measure for each of these null datasets. These treatment effect measures from the null datasets together provide an empirical estimate of the distribution of the treatment effect measure under H_0 for that method. Subsequently, a p -value is computed for the treatment effect measure captured under $H_1(S_{affected})$. This process is repeated many times (300 in our experiments), where each time we 1) generate a random $S_{affected}$, 2) generate a random dataset under $H_1(S_{affected})$ and compute each method’s treatment effect measure, and 3) generate 1000 copies of the dataset with no treatment effect to compute each method’s treatment effect measure distribution under H_0 . This process creates 300 p -values for each method which describe how extreme each of the $S_{affected}$ appear under H_0 . A method rejects H_0 for a given p -value if it is less than or equal to some test-level γ , corresponding to the $1 - \gamma$ quantile of the null distribution ($\gamma = 0.05$ in our experiments). Therefore, the detection power $P(Reject\ H_0 \mid H_1(S_{affected}))$ is captured as the proportion of p -values that are sufficiently extreme that they lead to the rejection of H_0 at level γ .

5.2.2 Detection Accuracy

While detection power measures how well a method identifies the presence of a subpopulation with a treatment effect $S_{affected}$, as compared to datasets with no treatment effect, detection accuracy measures how well a method can precisely and completely identify the affected subpopulation $S_{affected}$. Accurately identifying in which subpopulation(s) a treatment effect exists can be crucial, particularly when there is no prior theory to guide which subpopulations to inspect, or when the goal itself is to develop intuition for new theory. As described in §5.2, each of the methods we consider is able to return the subpopulation that

it determines as having the most statistically significant treatment effect S_{detected} . Each method will pick out a set of covariate profiles, which could have coherent structure (as with TESS, Causal Tree, and Interaction Tree), or be an unstructured collection of individually significant covariate profiles (as with Causal Forest). To accommodate both types of subpopulations, we therefore define detection accuracy as

$$\text{accuracy} = \frac{|S_{\text{detected}} \cap S_{\text{affected}}|}{|S_{\text{detected}} \cup S_{\text{affected}}|} = \frac{\sum_{R_i} \mathbb{1}_{\{R_i \in S_{\text{detected}} \cap S_{\text{affected}}\}}}{\sum_{R_i} \mathbb{1}_{\{R_i \in S_{\text{detected}} \cup S_{\text{affected}}\}}}. \quad (13)$$

where R_i are records in the treatment group. This definition of accuracy, commonly known as the Jaccard coefficient, is intended to balance precision (i.e., what proportion of the detected subjects truly have a treatment effect) and recall (i.e., what proportion of the subjects with a treatment effect are correctly detected). We note that $0 \leq \text{accuracy} \leq 1$; high accuracy values correspond to a detected subset S_{detected} that captures many of the subjects with treatment effects and few or no subjects without treatment effects.

5.3 Simulation Results

Our first set of results involve a treatment effect that is a mean shift in a normal distribution: the null distribution $f_0 = N(0, 1)$ and the alternative $f_1 = N(\delta, 1)$, where δ captures the magnitude of the signal (treatment effect). Recall from §5.2 that there are three parameters that we can vary to change the size and magnitude of the signal. For our simulation, we specifically consider $\delta \in \{0.25, 0.5, \dots, 3.0\}$, $\text{num_covs} \in \{1, 2, \dots, 10\}$, and $\text{value_prob} \in \{0.1, 0.2, \dots, 0.9\}$; the former controls magnitude of the treatment effect, while the latter two control the concentration of the treatment effect (i.e., the expected size of the affected subpopulation). Instead of considering every combination, we select the middle value of each parameter interval as a reference point ($\delta = 1.5, \text{num_covs} = 5, \text{value_prob} = 0.5$) and measure performance changes for one parameter, while keeping the others fixed.

Figure 1a shows the changes in each method’s detection power performance as we vary each of the three parameters that contribute to the strength of the treatment effect. From each of the three graphs we observe that TESS consistently exhibits more power than (or equivalent to) the other methods. More importantly, TESS exhibits statistically significant improvements in power for the most challenging ranges of parameter values (i.e., more subtle signals). The top plot varies effect size (or δ), which is positively associated with signal strength and negatively associated with detection difficulty; for values 2.0 and below TESS has significantly higher detection power than the competing methods. The middle plot varies the number of covariates selected to have only a subset of values be affected (num_covs). This parameter is negatively associated with signal strength and positively associated with detection difficulty; for values 5 and above, TESS has significantly higher detection power. The bottom plot varies the expected proportion of values, for the selected covariates, which will be affected (value_prob). This parameter is positively associated with signal strength and negatively associated with detection difficulty; for values 0.5 and below TESS exhibits significantly higher detection power. We see that, for sufficiently strong signals (based on both signal magnitude and concentration), all methods are able to distinguish between experiments with and without a subpopulation exhibiting a treatment effect, while TESS provides significant advantages in detection power for weaker signals.

Figure 1b shows the changes in each method’s detection accuracy as we vary each of the three parameters that contribute to the strength of the treatment effect. From each of

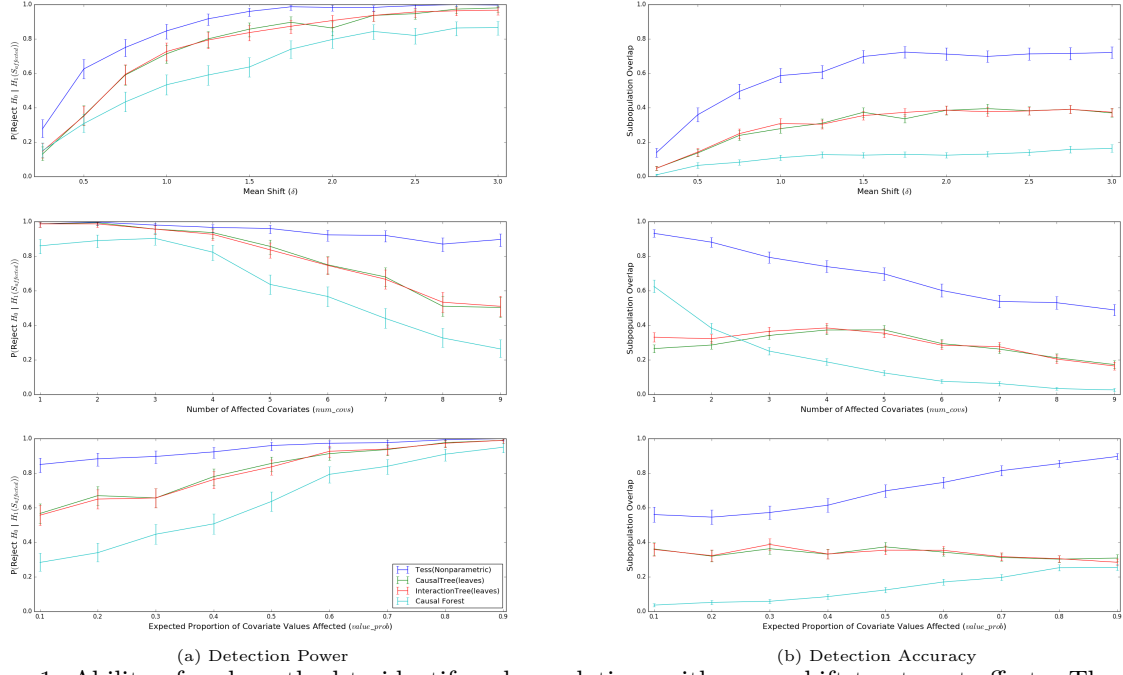


Figure 1: Ability of each method to identify subpopulations with mean shift treatment effects. The three parameters start as fixed ($\delta = 1.5$, $num_covs = 5$, $value_prob = 0.5$) and then are varied individually to see how detection ability varies.

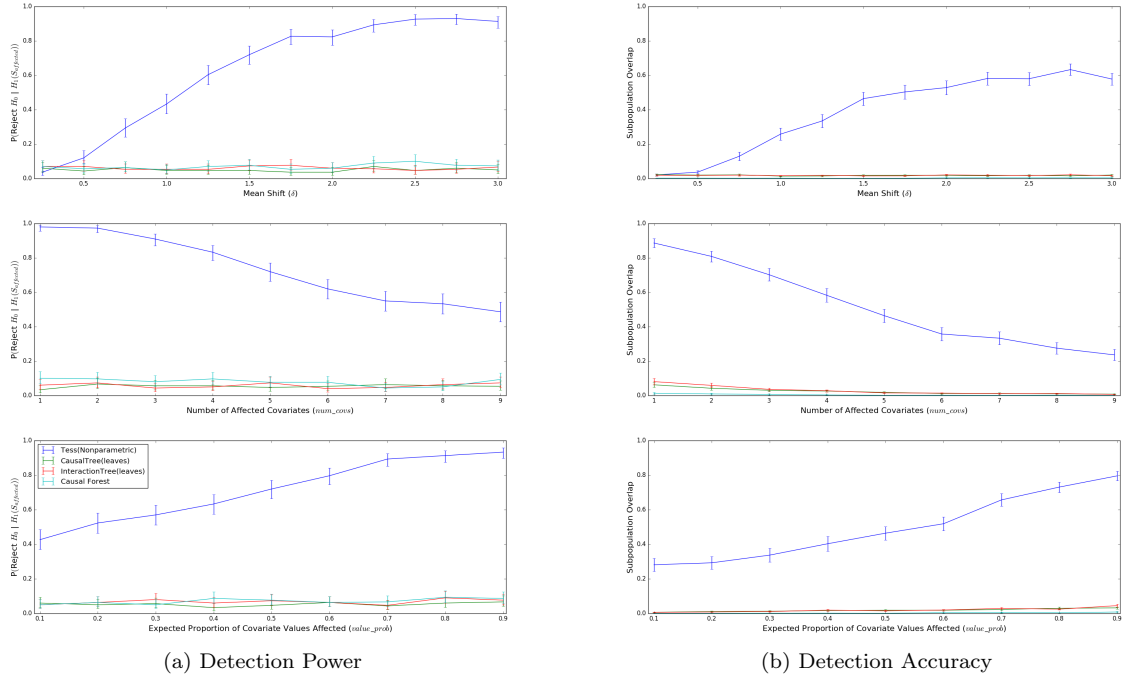


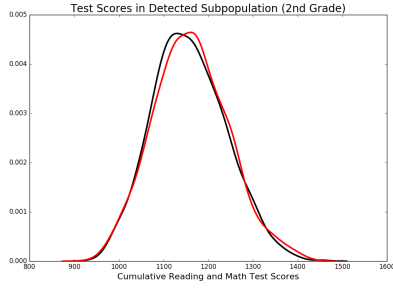
Figure 2: Ability of each method to identify subpopulations with an unaffected mean, but distributional treatment effect. The three parameters start as fixed ($\delta = 1.5$, $num_covs = 5$, $value_prob = 0.5$) and then are varied individually to see how detection ability varies.

the three graphs we observe that TESS consistently exhibits significantly higher accuracy than any other method. Recall that we measure subpopulation accuracy as in (13), which captures both precision and recall of the subpopulation returned by a method. The single tree methods tend to have high precision but low recall, resulting in compromised overall accuracy. Intuitively, these results indicate that the truly affected subpopulation is being spread over multiple leaves of the tree, despite its goal of partitioning the data into subpopulations with similar outcomes. This phenomenon may be caused by the greedy search aspect of tree learning: if the tree splits the affected subpopulation between two branches of the tree, the recall of any leaf will be compromised, especially when this split occurs close to the root of the tree. The Causal Forest ensemble method, on the other hand, exhibits relatively higher recall than precision. These results indicate that it is difficult for Causal Forest to distinguish between the covariate profiles that do and do not make up the truly affected subpopulation, as profiles from both sets appear to have statistically significant treatment effects. This inability stems from the fact that ensemble methods are designed to provide individual level predictions, therefore their conclusions regarding the statistical significance of a covariate profile are made in isolation from the other covariate profiles that also make up the affected subpopulation. Unlike single-tree methods, ensemble methods do not provide coherent and natural groupings of subpopulations. TESS, however, does provide a coherent subpopulation, which seems to balance precision and recall, maintaining a significantly higher subpopulation accuracy.

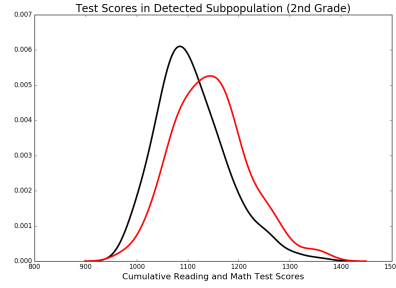
It is also important to note that the data generating process for these simulations (a treatment effect that occurs as a mean shift between treatment and control distributions) corresponds to the modeling assumptions of the current methods in the literature, which specifically attempt to detect mean shifts, while TESS is designed to detect more general distributional changes. TESS’s improved performance, as compared to the competing methods, in these adverse conditions may be due to its subset-scanning based approach, which combines information across groups of data in an attempt to find exactly and only the affected subset of data. Even if each individual covariate profile that is truly affected exhibits small evidence of a treatment effect, TESS can leverage the group structure and signal of all the affected covariate profiles, and correctly conclude that collectively the subpopulation exhibits significant evidence of a treatment effect. Additionally, the fact that TESS executes its optimization iteratively, unlike the greedy search of tree-based methods, enables it to rectify initial choices of subset that are later determined to be inferior.

Our second set of results considers treatment effects that do not align with the mean shift assumption that pervades the literature. Therefore, the null distribution is still $f_0 = N(0, 1)$; however, the alternative is a mixture distribution $f_1 = \frac{1}{2}N(-\delta, 1) + \frac{1}{2}N(\delta, 1)$. Here δ still captures the magnitude of the signal (treatment effect), and the remainder of the simulation process remains unchanged. This mixture distribution alternative, however, changes the detection task dramatically: while the average treatment effect is zero, there is still a clear difference in the outcome distribution between treated and control individuals.

Figure 2 shows how each method’s detection power and accuracy change as we vary each of three parameters that contribute to the strength of the treatment effect. If we compare these simulations to those above with a mean shift, TESS exhibits a consistent pattern of high performance, while the performance of the competing methods is dramatically lower. The detection power results indicate that, for the competing methods, it is hard to distinguish even strong distributional changes from random chance, while the accuracy

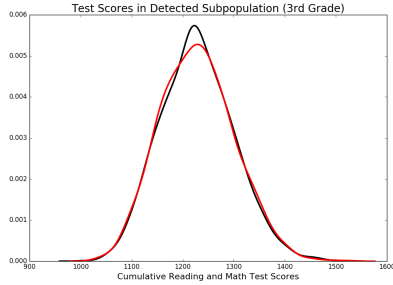


(a) All students in 2nd grade

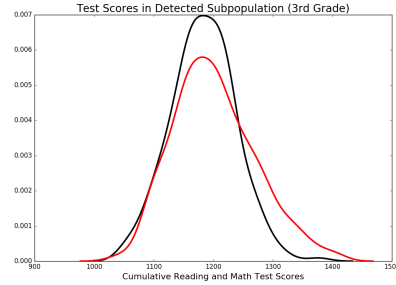


(b) Detected Subpopulation in 2nd grade

Figure 3: Kernel density plots of 2nd grade test scores for treatment students (red) who were in a regular classroom with a teacher’s aide and control students (black) who did not have a teacher’s aide.



(a) All students in 3rd grade



(b) Detected Subpopulation in 3rd grade

Figure 4: Kernel density plots of 3rd grade test scores for treatment students (red) who were in a regular classroom with a teacher’s aide and control students (black) who did not have a teacher’s aide.

results indicate that their pinpointing of the affected subpopulation is little better than random guessing. Given that there is no observable mean shift in these simulations, these results are consistent with what we expect: TESS is designed to identify more general distributional changes, while the other methods are unable to identify distributional changes without corresponding mean shifts.

5.4 A Case Study on Identifying Subpopulations: Tennessee STAR

There appears to be a consensus in the literature that the presence of a teaching aide in a regular-size classroom has an insignificant effect on test scores [53, 33, 19, 45]. (One significant effect was observed in first grade, but this effect was largely considered to be a false positive.) Therefore, we want to use TESS to compare regular classrooms with an aide to regular classrooms without an aide, to determine if there appears to be a subpopulation that was significantly and positively affected by the treatment. To do so, we replicated the analysis of the internal STAR team, using TESS to extend the results, with the goal of demonstrating what the STAR team could have surmised with present-day tools for uncovering heterogeneity. We replicate the original STAR analysis from [53, 45] which includes the sum of the Stanford math and reading scores as the outcome of interest. For the data provided to TESS for detection, we combine the panel data across years and include student’s grade level as a covariate. We would also like to obtain an unbiased estimate of the average treatment effect in the subpopulation identified by TESS. Therefore, we follow a cross-validation paradigm, where the entire dataset is partitioned into ten folds, and iteratively each fold is held out as a validation set (to obtain an estimate of the treatment effect) while the remaining nine folds are provided to TESS (for detection). We further partition the data into records corresponding to students observed in a regular classroom

	All (2 nd)	Detected (2 nd)	Undetected (2 nd)	All (3 rd)	Detected (3 rd)	Undetected (3 rd)
Treatment (std. dev.)	3.479 (2.547)	36.066*** (6.055)	1.309 (2.772)	-0.291 (2.277)	18.703*** (5.18)	0.1 (2.478)
P-value	0.172	<0.001	0.637	0.898	<0.001	0.968
Observations	4263	620	3643	4063	706	3357

Table 3: Table of estimated treatment effects on student test scores in 2nd and 3rd grade. *** indicates $p < 0.001$.

with an aide and a regular classroom without an aide, which serve as treatment and control groups respectively. In three of the ten folds, TESS identified exactly the same subset, which we will call the “detected subpopulation”. Essentially, this detected subpopulation is composed of students in second or third grade, who attended an inner-city or urban school, receiving instruction from a teacher with 10 or more years of experience¹⁰. Therefore, it appears that the presence of an aide raised the test-scores of students exhibiting the selected covariate values described above for grade, school type, and teacher experience, in addition to any values for gender, free-lunch status, teacher ethnicity, and teacher degree. The subpopulations that were returned in each of the ten folds exhibited a large amount of agreement with the detected subpopulation: the fold subpopulations exhibited 88% agreement (on average) with the detected subpopulation on the detection status of a record. The estimated average treatment effect for this detected subpopulation, averaged across all validation folds, is approximately a 34.19 point increase in total test score (36.45 and 22.28 for second and third grades respectively).

Given this consistency across folds, we use the full data to better understand the effect in the detected subpopulation generally. Table 3 shows the evaluation of the treatment effect for all second-grade students (column 1), second-grade students in the detected subpopulation (column 2), and second-grade students in the complement of the detected subpopulation (column 3). Additionally, Figure 3 shows the kernel density plots of the cumulative scores for all second-grade students and students in the detected subpopulation respectively. Figure 3a depicts a strong similarity in the distribution of all second graders’ scores with and without a full-time aide; there is a slight difference around the center of the distribution, but its magnitude is not sufficiently large to be significant, as seen by column 1 of Table 3. Conversely, Figure 3b depicts a difference in test scores for the detected subpopulation of second graders: there appears to be a clear effect of the treatment (dominated by a large mean shift), supported by column 2 of Table 3. We conduct a similar analysis with third graders, and observe similar results in Figure 4 and Table 3. However, the effect of the treatment in third grade appears to result in less of a mean shift, and is better characterized by a change in the skew (third moment) and therefore, the overall form of the distribution (Figure 4b). We note that because TESS is able to identify effects that change the distribution (and therefore higher order moments) of test scores, even if the difference in mean score between treatment and control students in third grade was smaller, TESS could potentially still identify the existence of a treatment effect.

There appears to be another consensus in the literature that small classrooms have a consistent, positive, and significant effect [53, 33, 19]; therefore, we also compare small classrooms to regular classrooms, and determine whether there appears to be a subpopulation which is the main driver of this effect. We conduct an analysis as above but with

¹⁰The detected subpopulation excluded teacher experience between 25 and 30 years. Including this range yields qualitatively the same results and conclusions.

STAR data records corresponding to students observed in a small classroom (treatment group) and a regular classroom (control group). For this analysis, TESS identified the entire population, which is congruent with the previous literature’s analysis of the consistent and significant average treatment effect in each grade. This result from TESS appears to indicate that the effect of small classroom size was not limited to a specific subpopulation. For both TESS analyses, we also conducted permutation testing to compensate for multiple hypothesis testing. Based on these results, we conclude that there is a less than 0.01% chance we would obtain a subpopulation with a score as extreme under the null hypothesis.

The detected subpopulation in the classrooms with aides is not only statistically significant, but may also provide domain insight into the efficacy of full-time aides. A possible explanation for the effect we observe in the detected subpopulation is the fact that 13 schools were chosen at random to have teachers participate in an in-service training session, which the literature has also deemed ineffective [53]. More specifically, 57 teachers were selected each summer from these schools to participate in a three-day in-service to help them teach more effectively in whatever class type they were assigned to; part of the instruction focused on how to work with an aide and also had the aides present. We note that the in-service only occurred during the summers prior to 2nd and 3rd grade, which are the grades identified by TESS. Therefore, it is possible that when provided proper training, the combination of an aide and an experienced teacher can provide a significantly enhanced education environment even in the challenging teaching environments that exist in inner-city and urban schools. An additional explanation is that the educational benefits may be cumulative—i.e., in each additional year a student in this subpopulation has access to the combination of an aide and experienced teacher, the treatment effect compounds—similar to what has been demonstrated in small classrooms for the overall population [33]. However, unlike in small classrooms, for this subpopulation in regular classrooms with an aide, the effects were not large enough to be distinguishable from zero (given the much smaller sample size of the affected subpopulation and smaller treatment effect) until after two years. While a more detailed follow-up analysis of these hypotheses might reveal other causal mechanisms at work, we believe that these results do present evidence that a treatment previously believed to be ineffective may actually have been effective for a particularly vulnerable subpopulation. Therefore, this analysis provides a sense of how TESS can be used as a tool for data-driven hypothesis generation in real-world policy analysis.

6 Conclusions

This paper has presented several contributions to the literature on statistical machine learning approaches for heterogeneous quantile treatment effects. Specifically, we detect the existence of a subpopulation for which the conditional quantile treatment effect (CQTE) is non-zero. This allows detection of treatment effects that manifest as arbitrary effects on the potential outcome distributions (or specific quantiles), rather than being limited to detection of mean shifts. Furthermore, we consider the challenge of identifying whether any subpopulation has been affected by treatment, and precisely characterizing the affected subpopulation, as opposed to the more typical problem setting of estimating individual-level treatment effects. We formalize the identification of subpopulations with significant treatment effects as an anomalous pattern detection problem, and present the Treatment Effect Subset Scan (TESS) algorithm, which serves as a computationally efficient test

statistic for the maximization of CQTE over all subpopulations. We demonstrate that the estimator used by TESS satisfies the linear-time subset scanning property, allowing it to be efficiently and exactly optimized over subsets of a covariate’s values, while evaluating only a linear rather than exponential number of subsets. This efficient conditional optimization step is incorporated into an iterative procedure which jointly maximizes over subsets of values for each covariate in the data: the result is a subpopulation, described as a subset of values for each covariate, which demonstrates the most evidence for a statistically significant treatment effect. In addition to its computational efficiency, we derive desirable statistical properties for the TESS estimator: bounded asymptotic probability of Type I and Type II errors under the sharp null hypothesis of no treatment effect, as well as providing sufficient conditions under the alternative hypothesis that will result in TESS exactly identifying the affected subpopulation. These properties apply more generally to the class of nonparametric scan statistics upon which TESS is built; therefore, this theory also provides additional contributions to the anomalous pattern detection, scan statistics, and goodness-of-fit literatures.

In addition to proposing a novel algorithm with desirable properties, we provide an extensive comparison between TESS and other recently proposed statistical machine learning methods for heterogeneous treatment effects (Causal Tree, Interaction Tree, and Causal Forest) through semi-synthetic simulations. Our results indicate that TESS consistently outperforms the other methods in its ability to identify and precisely characterize subpopulations which exhibit treatment effects. TESS significantly outperforms competing methods in the challenging scenarios where the treatment effect signal is weak (i.e., the signal magnitude is low or the affected subpopulation is small) because the subset scanning approach allows it to combine subtle signals across various dimensions of data in order to identify effects of interest. Moreover, TESS’s detection performance is consistent even when the treatment outcome distribution in the affected subpopulation has the same mean as the control outcome distribution, while the competing methods demonstrate essentially no ability to identify the affected subpopulation in the absence of a mean shift.

After demonstrating TESS’s performance through simulation, we explore the well-known Tennessee STAR experiment, searching for previously unidentified subpopulations with significant treatment effects. As a result of this analysis, TESS uncovered an intuitive subpopulation that seems to have experienced extremely significant improved test scores as a result of having a teacher’s aide in the classroom, a treatment that has consistently been considered ineffective (as measured by the average treatment effect) by the literature on the Tennessee STAR. This provides a sense of how TESS can be utilized as a tool for generating hypotheses to be further explored and tested. We do however caution researchers to view algorithms like TESS not as a replacement, but rather an assistive tool, for developing scientific and behavioral theory. Results discovered by these methods should be investigated further and evaluated to develop a deeper theoretical understanding of the phenomena they uncover. When used to this end, these tools fill a critical void: in many contexts it is rare to know *a priori* which hypotheses are relevant and supported by data, and the use of traditional methods (e.g., regression) puts the onus on the researcher to know which hypothesis to test. This process necessitates that theory comes first, and subsequent investigation is a form of confirmatory analysis. However, such a process can become an impediment to data-driven discovery: there is an increasing need for scalable methods to use (big) data to generate new hypotheses, rather than just confirming pre-existing beliefs.

In the late 1970s, John W. Tukey began to outline his vision for the future of statistics, which included a symbiotic relationship between exploratory and confirmatory data analysis. He argues these two forms of data analysis “can—and should—proceed side by side” [48] because he believed ideas “come from previous exploration more often than from lightning strokes” [49]. To this end Tukey advocates for using data to suggest hypotheses to test, or what we now call data-driven hypothesis generation. We see our work as the natural evolution of Tukey’s vision of data analysis: we develop an approach—rigorously conducted and theoretically grounded—to conduct exploratory analysis in randomized experiments, with the hope of catalyzing “lightning strokes” of discovery and the advancement of science.

References

- [1] A. Abadie, J. Angrist, and G. Imbens. Instrumental Variables Estimates of the Effect of Subsidized Training on the Quantiles of Trainee Earnings. *Econometrica*, 70(1):91–117, 2002.
- [2] M. L. Anderson. Multiple inference and gender differences in the effects of early intervention: A reevaluation of the Abecedarian, Perry preschool, and Early Training projects. *Journal of the American Statistical Association*, 103:1481–1495, Dec 2008.
- [3] J. D. Angrist and J.-S. Pischke. *Mostly Harmless Econometrics: An Empiricist’s Companion*. Princeton University Press, Dec 2008.
- [4] E. Arias-Castro, R. M. Castro, E. Tánzos, and M. Wang. Distribution-free detection of structured anomalies: Permutation and rank-based scans. *Journal of the American Statistical Association*, 0(ja):0–0, 2017.
- [5] S. F. Assmann, S. J. Pocock, L. E. Enos, and L. E. Kasten. Subgroup analysis and other (mis)uses of baseline data in clinical trials. *The Lancet*, 355:1064–1069, 2000.
- [6] S. Athey and G. Imbens. Recursive partitioning for heterogeneous causal effects. *Proceedings of the National Academy of Sciences*, 113(27):7353–7360, Jul 2016.
- [7] S. Athey, J. Tibshirani, and S. Wager. Generalized random forests. *The Annals of Statistics*, 47(2):1148–1178, Apr 2019.
- [8] S. Athey and S. Wager. Policy learning with observational data, 2020.
- [9] W. S. Barnett. Benefit-cost analysis of the Perry preschool program and its policy implications. *Educational evaluation and policy analysis*, 7(4):333–342, Jan 1985.
- [10] R. H. Berk and D. H. Jones. Goodness-of-fit test statistics that dominate the Kolmogorov statistics. *Zeitschrift für Wahrscheinlichkeitstheorie und Verwandte Gebiete*, 47:47–59, 1979.
- [11] F. Chen and D. B. Neill. Non-parametric scan statistics for event detection and forecasting in heterogeneous social media graphs. In *Proceedings of the 20th ACM SIGKDD International Conference on Knowledge Discovery and Data Mining*, KDD ’14, pages 1166–1175, 2014.

- [12] V. Chernozhukov, M. Demirer, E. Duflo, and I. Fernandez-Val. Generic machine learning inference on heterogeneous treatment effects in randomized experiments. Technical report, National Bureau of Economic Research, 2018.
- [13] V. Chernozhukov, I. Fernández-Val, and B. Melly. Inference on counterfactual distributions. *Econometrica*, 81(6):2205–2268, 2013.
- [14] V. Chernozhukov and C. Hansen. An IV Model of Quantile Treatment Effects. *Econometrica*, 73(1):245–261, 2005.
- [15] J. N. Cohn, D. G. Archibald, S. Ziesche, and Others. Effect of vasodilator therapy on mortality in chronic congestive heart failure. *New England Journal of Medicine*, 314(24):1547–1552, Jun 1986.
- [16] J. N. Cohn, G. Johnson, S. Ziesche, and Others. A comparison of enalapril with hydralazine–isosorbide dinitrate in the treatment of chronic congestive heart failure. *New England Journal of Medicine*, 325(5):303–310, Aug 1991.
- [17] A. Dvoretzky, J. Kiefer, and J. Wolfowitz. Asymptotic minimax character of the sample distribution function and of the classical multinomial estimator. *The annals of mathematical statistics*, 27(3):642–669, Sep 1956.
- [18] S. Firpo. Efficient Semiparametric Estimation of Quantile Treatment Effects. *Econometrica*, 75(1):259–276, 2007.
- [19] J. Folger and C. Breda. Evidence from project STAR about class size and student achievement. *Peabody Journal of Education*, 67(1):17–33, Sep 1989.
- [20] J. C. Foster, J. M. G. Taylor, and S. J. Ruberg. Subgroup identification from randomized clinical trial data. *Statistics in medicine*, 30(24):2867–2880, Aug 2011.
- [21] J. H. Friedman. Multivariate adaptive regression splines. *Annals of Statistics*, 19(1):1–67, Mar 1991.
- [22] P. Gaenssler and J. A. Wellner. *Glivenko–Cantelli Theorems*. John Wiley & Sons, Inc., Hoboken, NJ, USA, Jul 2004.
- [23] D. P. Green and H. L. Kern. Modeling heterogeneous treatment effects in survey experiments with Bayesian additive regression trees. *Public Opinion Quarterly*, 76(3):491–511, Sep 2012.
- [24] J. Grimmer, S. Messing, and S. J. Westwood. Estimating heterogeneous treatment effects and the effects of heterogeneous treatments with ensemble methods. *Political Analysis*, 25(4):413–434, 2017.
- [25] J. L. Hill. Bayesian nonparametric modeling for causal inference. *Journal of Computational and Graphical Statistics*, 20(1):217–240, Jan 2011.
- [26] K. Imai and M. Ratkovic. Estimating treatment effect heterogeneity in randomized program evaluation. *The Annals of Applied Statistics*, 7(1):443–470, Mar 2013.

- [27] L. Jager and J. A. Wellner. Goodness-of-fit tests via phi-divergences. *The Annals of Statistics*, 35(5):2018–2053, Oct 2007.
- [28] J. Keilson and H. Ross. First passage time of gaussian markov (ornstein-uhlenbeck) statistical processes. *Selected Tables in mathematical studies*, 3:233–327, 1975.
- [29] T. Kitagawa and A. Tetenov. Who should be treated? empirical welfare maximization methods for treatment choice. *Econometrica*, 86(2):591–616, 2018.
- [30] R. Koenker. Nonparametrics and Robustness in Modern Statistical Inference and Time Series Analysis: A Festschrift in honor of Professor Jana Jurečková. *Institute of Mathematical Statistics Collections*, pages 134–142, 2010.
- [31] R. Koenker and G. Bassett Jr. Regression quantiles. *Econometrica: journal of the Econometric Society*, pages 33–50, 1978.
- [32] R. Kohavi, A. Deng, B. Frasca, T. Walker, Y. Xu, and N. Pohlmann. Online controlled experiments at large scale. In *Proceedings of the 19th ACM SIGKDD International Conference on Knowledge Discovery and Data Mining*, New York, NY, USA, 2013.
- [33] A. B. Krueger. Experimental estimates of education production functions. *Quarterly Journal of Economics*, 114(2):497–532, May 1999.
- [34] E. Mbakop and M. Tabord-Meehan. Model selection for treatment choice: Penalized welfare maximization, 2020.
- [35] E. McFowland III, S. D. Speakman, and D. B. Neill. Fast generalized subset scan for anomalous pattern detection. *The Journal of Machine Learning Research*, 14(1):1533–1561, Jun 2013.
- [36] N. Meinshausen. Quantile regression forests. *The Journal of Machine Learning Research*, 7(1):983–999, Jun 2006.
- [37] R. Miller and D. Siegmund. Maximally Selected Chi Square Statistics. *Biometrics*, 38(4):1011, 1982.
- [38] D. B. Neill. Fast subset scan for spatial pattern detection. *Journal of the Royal Statistical Society (Series B: Statistical Methodology)*, 74(2):337–360, 2012.
- [39] D. B. Neill, E. McFowland III, and H. Zheng. Fast subset scan for multivariate event detection. *Statistics in medicine*, 32(13):2185–2208, 2013.
- [40] B. Nye, L. V. Hedges, and S. Konstantopoulos. The effects of small classes on academic achievement: The results of the Tennessee class size experiment. *American Educational Research Journal*, 37(1):123–151, 2000.
- [41] S. Saul. F.D.A. Approves a Heart Drug for African-Americans, June 2005. <https://www.nytimes.com/2005/06/24/health/fda-approves-a-heart-drug-for-africanamericans.html> (Accessed: 06-05-2018).

- [42] V. Schiele and H. Schmitz. Quantile treatment effects of job loss on health. *Journal of Health Economics*, 49:59–69, 2016.
- [43] L. J. Schweinhart, H. V. Barnes, and D. P. Weikart. Significant benefits: The High/Scope Perry preschool study through age 27. Technical Report 10, High/Scope Educational Research Foundation, 1993.
- [44] G. R. Shorack and J. A. Wellner. *Empirical Processes with Applications to Statistics*. Society for Industrial and Applied Mathematics, May 1986.
- [45] J. Stock and M. Watson. *Introduction to Econometrics 2nd edition*. Pearson, 2007.
- [46] X. Su, C.-L. Tsai, H. Wang, D. M. Nickerson, and B. Li. Subgroup analysis via recursive partitioning. *Journal of Machine Learning Research*, 10:141–158, Dec 2009.
- [47] L. Tian, A. A. Alizadeh, A. J. Gentles, and R. Tibshirani. A simple method for estimating interactions between a treatment and a large number of covariates. *Journal of the American Statistical Association*, 109(508):1517–1532, Dec 2014.
- [48] J. W. Tukey. *Exploratory Data Analysis*. Addison-Wesley Publishing Company, 1977.
- [49] J. W. Tukey. We need both exploratory and confirmatory. *The American Statistician*, 34(1), 1980.
- [50] S. Vansteelandt, M. Joffe, et al. Structural nested models and g-estimation: the partially realized promise. *Statistical Science*, 29(4):707–731, 2014.
- [51] S. Wager and S. Athey. Estimation and inference of heterogeneous treatment effects using random forests. *Journal of the American Statistical Association*, 113(523):1228–1242, 2018.
- [52] H. I. Weisberg and V. P. Pontes. Post hoc subgroups in clinical trials: Anathema or analytics? *Clinical trials*, 12(4):357–364, Aug 2015.
- [53] E. R. Word, J. Johnston, H. P. Bain, and Others. The state of Tennessee’s Student/Teacher Achievement Ratio (STAR) project: Technical report 1985–1990. *Nashville: Tennessee State Department of Education*, 1990.
- [54] Z. Zhou, S. Athey, and S. Wager. Offline multi-action policy learning: Generalization and optimization, 2018.

A Score Functions

To begin we revisit the general form of the score function—or equivalently the quantile treatment effect test statistic—that we refer to as the nonparametric scan statistic. Additionally, we establish equivalences, as different forms will lend themselves to various proof strategies we implement later.

$$\begin{aligned} \max_S F(S) &= \max_{S,\alpha} F_\alpha(S) &&= \max_{S,\alpha,\beta} F_{\alpha,\beta}(S) \\ &= \max_{S,\alpha} \Delta(\alpha, N_\alpha(S), N(S)) = \max_{S,\alpha,\beta} \sum_{x \in U_X(S)} \omega(\alpha, \beta, N_\alpha(x), N(x)). \end{aligned} \quad (14)$$

To motivate the use of our score function to evaluate the quantile treatment effect in subpopulation S , we will first demonstrate that simply maximizing the original conditional quantile treatment effect,

$$\max_S \max_\alpha \mathbb{F}_{Y(1)|X \in S}^{-1}(\alpha) - \mathbb{F}_{Y(0)|X \in S}^{-1}(\alpha),$$

is unproductive as it reduces to the trivial solution of a singular covariate profile.

Proposition 1. *If $(S^*, \alpha^*) = \arg \max_{S \subseteq D, \alpha} \mathbb{F}_{Y(1)|X \in S}^{-1}(\alpha) - \mathbb{F}_{Y(0)|X \in S}^{-1}(\alpha)$ and $x^* = \arg \max_{x \in D} \mathbb{F}_{Y(1)|X=x}^{-1}(\alpha^*) - \mathbb{F}_{Y(0)|X=x}^{-1}(\alpha^*)$, then $S^* = x^*$.*

Proof. First let $S \subseteq D$ be any fixed subpopulation in our experimental data D , and $\alpha \in (0, 1)$ be a fixed quantile. Next we re-write a (potential outcomes) distribution as follows:

$$\begin{aligned} \mathbb{F}_{Y|X \in S}(y) &= \frac{\mathbb{F}_{Y,X \in S}(y)}{F(X \in S)} \\ &= \frac{P(Y \leq y, X \in S)}{P(X \in S)} \\ &= \frac{\sum_{x \in S} P(\{Y \leq y, X = x\})}{P(X \in S)} \\ &= \sum_{x \in S} P(Y \leq y | X = x) P(X = x | x \in S). \end{aligned}$$

This allows us to also rewrite the (potential outcomes) quantile function as follows:

$$\begin{aligned} \mathbb{F}_{Y|X \in S}^{-1}(\alpha) &= \sum_{x \in S} \inf_y \{y : P(Y \leq y | X = x) \geq \alpha\} P(X = x | x \in S) \\ &= \sum_{x \in S} \mathbb{F}_{Y|X=x}^{-1}(\alpha) P(X = x | x \in S). \end{aligned}$$

Therefore, if we define

$$Q_x(\alpha) = \mathbb{F}_{Y(1)|X=x}^{-1}(\alpha) - \mathbb{F}_{Y(0)|X=x}^{-1}(\alpha)$$

then

$$\begin{aligned} \mathbb{F}_{Y(1)|X \in S}^{-1}(\alpha) - \mathbb{F}_{Y(0)|X \in S}^{-1}(\alpha) &= \sum_{x \in S} Q_x(\alpha) P(X = x | x \in S) \\ &\leq \max_{x \in S} Q_x(\alpha), \end{aligned}$$

where the inequality follows from the fact that $\sum_{x \in S} P(X = x | x \in S) = 1$. Moreover, because this inequality holds $\forall S, \alpha$, then it also must hold for S^*, α^* . Therefore, we finally have

$$\max_{S \subseteq D} \mathbb{F}_{Y(1)|X \in S}^{-1}(\alpha^*) - \mathbb{F}_{Y(0)|X \in S}^{-1}(\alpha^*) \leq \max_{x \in S \subseteq D} Q_x(\alpha) \quad (15)$$

$$= \max_{x \in S \subseteq D} Q_x(\alpha) \quad (16)$$

$$= \max_{x \in S} \mathbb{F}_{Y(1)|X=x}^{-1}(\alpha) - \mathbb{F}_{Y(0)|X=x}^{-1}(\alpha)$$

where (16) follows from the fact that the inequality in (15) must be a strict equality because $\{\max_{x \in S \subseteq D}\} \subseteq \{\max_{S \subseteq D}\}$. \square

Now that we demonstrated that the usefulness of maximizing the original conditional quantile effect measure is compromised by its reduction to a singular covariate profile, let us consider the treatment effect evaluation measure based on our nonparametric scan statistic, by first revisiting the score function. In the main text we introduced the Berk-Jones score function which assumes that the data generating process for each $N_\alpha(x)$ follows a binomial distribution and therefore computes the log-likelihood ratio statistic $F(S) = \log \left(\frac{P(\text{Data}|H_1(S))}{P(\text{Data}|H_0)} \right)$, which can be written as the product of the total number of p -values $N(S)$ in subset S and a divergence $Div \left(\frac{N_\alpha(S)}{N(S)}, \alpha \right)$ between the observed and expected proportions of p -values that are significant at level α . More specifically, we have:

$$\begin{aligned} H_0 : N_\alpha(x) &\sim \text{Binomial}(N(x), \alpha) \quad \forall x \\ H_1(S) : N_\alpha(x) &\sim \text{Binomial}(N(x), \beta) \quad \forall x \in S \quad \beta \neq \alpha, \end{aligned}$$

with the following Berk-Jones (BJ) log-likelihood ratio statistic [10]:

$$\begin{aligned} F_\alpha^{BJ}(S) &= \log \left[\frac{P(\text{Data}|H_1(S))}{P(\text{Data}|H_0)} \right] \\ &= N_\alpha(S) \log \left(\frac{\beta}{\alpha} \right) + (N(S) - N_\alpha(S)) \log \left(\frac{1-\beta}{1-\alpha} \right) \\ &= N(S) Div_{KL} \left(\frac{N_\alpha(S)}{N(S)}, \alpha \right), \end{aligned}$$

where we have used the maximum likelihood estimate $\beta = \beta_{\text{mle}}(S) = \frac{N_\alpha(S)}{N(S)}$, and $Div_{KL}(\cdot, \cdot)$ is the Kullback-Leibler divergence, $Div_{KL}(x, y) = x \log \frac{x}{y} + (1-x) \log \frac{1-x}{1-y}$

We now also introduce the Normal-Approximation score function, which is based on the normal approximation to the binomial data generating process assumed in Berk-Jones:

$$\begin{aligned} H_0 : N_\alpha(x) &\sim \text{Gaussian}(N(x)\alpha, \alpha(1-\alpha)N(x)) \quad \forall x \\ H_1(S) : N_\alpha(x) &\sim \text{Gaussian}(N(x)\beta, \alpha(1-\alpha)N(x)) \quad \forall x \in S \quad \beta \neq \alpha, \end{aligned}$$

with the following normal approximation (NA) log-likelihood ratio statistic:

$$\begin{aligned}
F_\alpha^{NA}(S) &= \log \left[\frac{P(\text{Data}|H_1(S))}{P(\text{Data}|H_0)} \right] \\
&= \frac{N_\alpha(S)(\beta - \alpha)}{\alpha(1 - \alpha)} + \frac{N(S)(\alpha^2 - \beta^2)}{2\alpha(1 - \alpha)} \\
&= \frac{(N_\alpha(S) - N(S)\alpha)^2}{2N(S)\alpha(1 - \alpha)} \\
&= N(S) \text{Div}_{\frac{1}{2}\chi^2} \left(\frac{N_\alpha(S)}{N(S)}, \alpha \right).
\end{aligned}$$

where we have again used the maximum likelihood estimate of $\beta = \frac{N_\alpha(S)}{N(S)}$, and $\text{Div}_{\frac{1}{2}\chi^2}(\cdot, \cdot)$ is a scaled χ^2 divergence, $\text{Div}_{\frac{1}{2}\chi^2}(x, y) = \frac{(x-y)^2}{2y(1-y)}$.

The first result we show is that in the limit F^{BJ} is well approximated by F^{NA} , which will then allow us to focus the remainder of our theoretical results on F^{NA} specifically.

Proposition 2. $F^{BJ}(S) \asymp F^{NA}(S)$ as $N(S) \rightarrow \infty$.

Proof. Recall that $K(x, y) = \text{Div}_{KL}(x, y) = x \log \frac{x}{y} + (1-x) \log \frac{1-x}{1-y}$. By expanding $K(x, y)$ through a Taylor series, we have

$$\begin{aligned}
K(x, y) &= K(y, y) + \left. \frac{\partial K(x, y)}{\partial x} \right|_{x=y} (x - y) + \left. \frac{\partial^2 K(x, y)}{\partial^2 x} \right|_{x=y'} \frac{(x - y)^2}{2} \\
&= 0 + 0 + \frac{(x - y)^2}{2y'(1 - y')}
\end{aligned}$$

for some y' such that $|y' - x| \leq |y - x|$. Therefore,

$$\begin{aligned}
F^{BJ}(S) &= \max_\alpha N(S) K \left(\frac{N_\alpha(S)}{N(S)}, \alpha \right) \\
&= \max_\alpha N(S) \frac{\left(\frac{N_\alpha(S)}{N(S)} - \alpha \right)^2}{2\alpha'(1 - \alpha')} \quad \left(\text{where } \left| \alpha' - \frac{N_\alpha(S)}{N(S)} \right| \leq \left| \alpha - \frac{N_\alpha(S)}{N(S)} \right| \right) \\
&\leq \max_\alpha N(S) \left[\frac{\left(\frac{N_\alpha(S)}{N(S)} - \alpha \right)^2}{2\alpha(1 - \alpha)} \vee \frac{\left(\frac{N_\alpha(S)}{N(S)} - \alpha \right)^2}{2\frac{N_\alpha(S)}{N(S)} \left(1 - \frac{N_\alpha(S)}{N(S)} \right)} \right]
\end{aligned}$$

and

$$\geq \max_\alpha N(S) \left[\frac{\left(\frac{N_\alpha(S)}{N(S)} - \alpha \right)^2}{2\alpha(1 - \alpha)} \wedge \frac{\left(\frac{N_\alpha(S)}{N(S)} - \alpha \right)^2}{2\frac{N_\alpha(S)}{N(S)} \left(1 - \frac{N_\alpha(S)}{N(S)} \right)} \right].$$

Furthermore, under H_0 , $\frac{N_\alpha(S)}{N(S)} \xrightarrow{a.s.} \alpha \implies \alpha' \xrightarrow{a.s.} \alpha$, which by the continuous mapping theorem results in

$$F^{BJ}(S) \xrightarrow{a.s.} \max_\alpha N(S) \frac{\left(\frac{N_\alpha(S)}{N(S)} - \alpha \right)^2}{2\alpha(1 - \alpha)} = F^{NA}(S).$$

However, under $H_1(S^T)$, $\frac{N_\alpha(S)}{N(S)} \xrightarrow{a.s.} \beta(\alpha)$, therefore asymptotically for $F^{BJ}(S)$ we have,

$$\begin{aligned} \max_{\alpha} N(S) \frac{\left(\frac{N_\alpha(S)}{N(S)} - \alpha\right)^2}{2\alpha(1-\alpha)} \left(1 \bigwedge \frac{\alpha(1-\alpha)}{\beta(\alpha)(1-\beta(\alpha))}\right) &\leq F^{BJ}(S) \\ &\leq \max_{\alpha} N(S) \frac{\left(\frac{N_\alpha(S)}{N(S)} - \alpha\right)^2}{2\alpha(1-\alpha)} \left(1 \bigvee \frac{\alpha(1-\alpha)}{\beta(\alpha)(1-\beta(\alpha))}\right). \end{aligned}$$

We can see that $F^{BJ}(S)$ is bounded above and below by either $F^{NA}(S)$ or a constant times $F^{NA}(S)$. \square

We also note that there are a collection of well-known supremum goodness-of-fit statistics used in the literature, all of which are described in [27], that can be written as a transformation of $F_\alpha^{NA}(S)$:

the Kolmogorov-Smirnov statistic

$$\begin{aligned} F^{KS}(S) &= \max_{\alpha} F_{\alpha}^{KS}(S) \\ &= \max_{\alpha} \frac{(N_{\alpha}(S) - N(S)\alpha)}{\sqrt{N(S)}} \\ &= \max_{\alpha} \sqrt{2\alpha(1-\alpha)F_{\alpha}^{NA}(S)}, \end{aligned}$$

the Cramer-von Mises statistic

$$\begin{aligned} F^{CV}(S) &= \max_{\alpha} F_{\alpha}^{CV}(S) \\ &= \max_{\alpha} \frac{(N_{\alpha}(S) - N(S)\alpha)^2}{N(S)} \\ &= \max_{\alpha} 2\alpha(1-\alpha)F_{\alpha}^{NA}(S), \end{aligned}$$

the Higher-Criticism statistic

$$\begin{aligned} F^{HC}(S) &= \max_{\alpha} F_{\alpha}^{HC}(S) \\ &= \max_{\alpha} \frac{(N_{\alpha}(S) - N(S)\alpha)}{\sqrt{N(S)\alpha(1-\alpha)}} \\ &= \max_{\alpha} \sqrt{2F_{\alpha}^{NA}(S)}, \end{aligned}$$

and the Anderson-Darling statistic

$$\begin{aligned} F^{AD}(S) &= \max_{\alpha} F_{\alpha}^{AD}(S) \\ &= \max_{\alpha} \frac{(N_{\alpha}(S) - N(S)\alpha)^2}{N(S)\alpha(1-\alpha)} \\ &= \max_{\alpha} 2F_{\alpha}^{NA}(S). \end{aligned}$$

As a result of this connection between F^{NA} and these other statistics, we have the following:

Proposition 3. *If S maximizes $F_\alpha^{NA}(S)$, then it maximizes $F_\alpha^{KS}(S)$, $F_\alpha^{CV}(S)$, $F_\alpha^{HC}(S)$ and $F_\alpha^{AD}(S)$.*

Proof. First, we note that $T(F_\alpha^{NA})$, where $T(x) = (bx)^a$, for $b \in \{1, 2, 2\alpha(1 - \alpha)\}$ and $a \in \{1, \frac{1}{2}\}$ is a monotonically increasing transformation. Therefore, $\arg \max_S F_\alpha^{NA}(S) = \arg \max_S T(F_\alpha^{NA}(S))$, because $\arg \max$ is invariant to monotone transformations. \square

We now show that assumptions (A1), (A2), and (A3) stated in §3.4.1 are satisfied by scoring functions $F_\alpha^{BJ}(S)$ and $F_\alpha^{NA}(S)$, as well as all of the other functions discussed above, given that they are monotone transformations of $F_\alpha^{NA}(S)$.

Proposition 4. *For a fixed value of α , $F_\alpha^{BJ}(S)$ is (1) monotonically increasing with respect to $N_\alpha(S)$, (2) monotonically decreasing with respect to $N(S)$, and (3) convex with respect to $N_\alpha(S)$ and $N(S)$.*

Proof. $F_\alpha^{BJ}(S)$ can be written as $N_\alpha(S) \log \left(\frac{N_\alpha(S)}{N(S)\alpha} \right) + (N(S) - N_\alpha(S)) \log \left(\frac{N(S) - N_\alpha(S)}{N(S) - N(S)\alpha} \right)$. $F_\alpha^{BJ}(S)$ is monotonically increasing w.r.t. $N_\alpha(S)$ because

$$\begin{aligned} \frac{\partial F_\alpha^{BJ}(S)}{\partial N_\alpha(S)} &= 1 + \log \left(\frac{N_\alpha(S)}{N(S)\alpha} \right) - 1 - \log \frac{N(S) - N_\alpha(S)}{N(S) - N(S)\alpha} \\ &= \log \left(\frac{N_\alpha(S)}{N(S)\alpha} \right) + \log \left(\frac{N(S) - N(S)\alpha}{N(S) - N_\alpha(S)} \right) \\ &= \log \left(\frac{\frac{N_\alpha(S)}{N(S)}}{1 - \frac{N_\alpha(S)}{N(S)}} \cdot \frac{1 - \alpha}{\alpha} \right) \\ &\geq 0. \end{aligned}$$

The last inequality is strict when $\frac{N_\alpha(S)}{N(S)} > \alpha$, and we define $F_\alpha^{BJ}(S) = 0$ otherwise.

Similarly, $F_\alpha^{BJ}(S)$ is monotonically decreasing w.r.t. $N(S)$ because

$$\begin{aligned} \frac{\partial F_\alpha^{BJ}(S)}{\partial N(S)} &= -\frac{N_\alpha(S)}{N(S)} + \log \left(\frac{N(S) - N_\alpha(S)}{N(S) - N(S)\alpha} \right) + \frac{N_\alpha(S)}{N(S)} \\ &= \log \left(\frac{N(S) - N_\alpha(S)}{N(S) - N(S)\alpha} \right) \\ &\leq 0. \end{aligned}$$

Again, the last inequality is strict when $\frac{N_\alpha(S)}{N(S)} > \alpha$, and we define $F_\alpha^{BJ}(S) = 0$ otherwise.

Finally, $F_\alpha^{BJ}(S)$ is convex in $N_\alpha(S)$ and $N(S)$ because it can be written as $N(S)f \left(\frac{N_\alpha(S)}{N(S)} \right)$, where $f(x) = x \log \frac{x}{\alpha} + (1 - x) \log \frac{1-x}{1-\alpha}$. $f(x)$ is a convex function, since $\frac{d^2 f}{dx^2} = \frac{1}{x} + \frac{1}{1-x} > 0$ for $x \in (0, 1)$. Then $F_\alpha^{BJ}(S)$ is convex since it is the perspective of a convex function. \square

Proposition 5. *For a fixed value of α , $F_\alpha^{NA}(S)$ is (1) monotonically increasing with respect to $N_\alpha(S)$, (2) monotonically decreasing with respect to $N(S)$, and (3) convex with respect to $N_\alpha(S)$ and $N(S)$.*

Proof. $F_\alpha^{NA}(S)$ can be written as $\frac{(N_\alpha(S)-N(S)\alpha)^2}{2N(S)\alpha(1-\alpha)}$. $F_\alpha^{NA}(S)$ is monotonically increasing w.r.t. $N_\alpha(S)$ as

$$\begin{aligned}\frac{\partial F_\alpha^{NA}(S)}{\partial N_\alpha(S)} &= \frac{\frac{N_\alpha(S)}{N(S)} - \alpha}{\alpha(1-\alpha)} \\ &\geq 0.\end{aligned}$$

The last inequality is strict when $\frac{N_\alpha(S)}{N(S)} > \alpha$, and we define $F_\alpha^{NA}(S) = 0$ otherwise.

Similarly, $F_\alpha^{NA}(S)$ is monotonically decreasing w.r.t. $N(S)$ as

$$\begin{aligned}\frac{\partial F_\alpha^{NA}(S)}{\partial N(S)} &= \frac{2N(S)^2\alpha^3(1-\alpha) - 2N_\alpha(S)^2\alpha(1-\alpha)}{4N(S)^2\alpha^2(1-\alpha)^2} \\ &= \frac{\alpha^2 - \left(\frac{N_\alpha(S)}{N(S)}\right)^2}{2\alpha(1-\alpha)} \\ &\leq 0,\end{aligned}$$

given $\alpha \in (0, 1)$. Again, the last inequality is strict when $\frac{N_\alpha(S)}{N(S)} > \alpha$, and we define $F_\alpha^{NA}(S) = 0$ otherwise.

Finally, $F_\alpha^{NA}(S)$ is convex in $N_\alpha(S)$ and $N(S)$ because it can be written as $N(S)f\left(\frac{N_\alpha(S)}{N(S)}\right)$, where $f(x) = \frac{(x-\alpha)^2}{2\alpha(1-\alpha)}$. $f(x)$ is a convex function, since $\frac{d^2f}{dx^2} = \frac{1}{\alpha(1-\alpha)} > 0$ for $\alpha \in (0, 1)$. Then $F_\alpha^{NA}(S)$ is convex since it is the perspective of a convex function. \square

B Supplementary Materials: Proofs of Lemmas and Theorems

In this section, we provide detailed proofs of the Lemmas and Theorems stated in the main text. Before presenting the proofs, we (re-)introduce notation that will be used throughout the proofs.

B.1 Notation

S^T : the truly affected (rectangular) subset.

S^* : the highest scoring (rectangular) subset, $\arg \max_{S \in \text{Rect}} F(S)$, where Rect is the set of all rectangular subsets in D .

α^* : the α at which S^* is highest scoring, i.e., $\arg \max_\alpha F_\alpha(S^*)$.

S_u^* : the highest scoring unconstrained subset, $\arg \max_{S \subseteq D} F(S)$.

α_u^* : the α at which S_u^* is highest scoring, i.e., $\arg \max_\alpha F_\alpha(S_u^*)$.

U_X : a function which returns the unique covariate profiles (non-empty tensor cells) in a set.

M : $|U_X(D)|$, the number of unique covariate profiles in our treatment data, or equivalently the number of cells with treatment observations in our data tensor.

k : $\frac{|U_X(S^T)|}{|U_X(D)|}$, the proportion of non-empty cells that are affected under $H_1(S^T)$.

$\beta(\alpha)$: $P(\hat{p}(y; x) \leq \alpha \mid H_1(S^T))$, for all the p -values of covariate profiles $x \in U_X(S^T)$.
 $h(\delta)$: the critical value for the test statistic, $\max_{S \in \text{Rect}} F(S)$, at a given Type-I error rate $\delta > 0$.
 ϕ : Probability density function of standard normal distribution.
 Φ : Cumulative distribution function of standard normal distribution.

Additionally, we will assume that each of the M non-empty tensor cells (or unique treatment profiles) contain exactly n p -values, for mathematical convenience. We are interested in the distribution of the score $\max_S F(S)$ under the null hypothesis H_0 , assuming that all p -values are uniformly distributed on $[0, 1]$, and under the alternative hypothesis $H_1(S^T)$, assuming that there exist some constants α and β such that $\Pr(\hat{p} < \alpha) = \beta$ in subset S^T , for $\beta > \alpha$. We assume that a constant fraction of cells k , $0 < k \leq 1$, are affected under H_1 .

B.2 Statistical Properties

We now demonstrate desirable statistical properties of $\max_{S \in \text{Rect}} F(S)$. Our derivations are based on $F^{NA}(S)$, but we show that these properties also extend to $F^{BJ}(S)$, our statistic of choice in the main text, and many other statistics because of their close relationship with $F^{NA}(S)$, as described in Appendix A. More specifically, we demonstrate that, using $\max_{S \in \text{Rect}} F(S)$ as a test statistic of the data, we can appropriately (fail to) reject H_0 with high probability. For mathematical convenience, the results derived in this section assume that $N(x) = n$ for all $x \in U_X(D)$, i.e., each unique covariate profile in the data has exactly n data points (and therefore n p -values). We also assume under the alternative hypothesis $H_1(S^T)$ that a constant fraction of cells k , $0 < k \leq 1$, are affected. Finally, we consider the asymptotic regime where $n \rightarrow \infty$. Ultimately, we will show that for any Type I error rate $\delta > 0$, we can compute a critical value $h(\delta)$ such that we have the following:

$$\begin{aligned}
 \lim_{n \rightarrow \infty} P_{H_0} \left(\max_{S \in \text{Rect}} F(S) > h(\delta) \right) &\leq \delta, \\
 \lim_{n \rightarrow \infty} P_{H_1} \left(\max_{S \in \text{Rect}} F(S) > h(\delta) \right) &= 1.
 \end{aligned}$$

We begin by first recognizing that $F(S^*) \leq F(S_u^*)$, i.e., the score of the optimal rectangular subset is upper bounded by the score of optimal unconstrained subset, because the space of rectangular subsets is contained within the space of all subsets. Consequently, the distribution $F(S_u^*)$ under H_0 provides an upper bound on the distribution of $F(S^*)$ under H_0 . Therefore, we will begin by establishing a distributional upper bound on $\sqrt{F(S_u^*)}$ under H_0 , which by transitivity will also provide an upper bound on the distribution of $\sqrt{F(S^*)}$.

Lemma 1. *Under H_0 defined in (12), let $N(x) = n \forall x \in U_X(D)$, then as $n \rightarrow \infty$,*

$$\begin{aligned}
 \sqrt{F(S_u^*)} &\xrightarrow{d} G(\mathbb{W}(\alpha_{\min}, \alpha_{\max}), M) \\
 &\leq C\sqrt{M} + \frac{\mathbb{W}(\alpha_{\min}, \alpha_{\max})}{\sqrt{2}},
 \end{aligned}$$

where the function G and constant $C < 1$ are known; $\mathbb{W}(\alpha_{\min}, \alpha_{\max}) = \sup_{\alpha \in [\alpha_{\min}, \alpha_{\max}]} \frac{|B(\alpha)|}{\sqrt{\alpha(1-\alpha)}}$, and $B(\alpha)$ represents a Brownian bridge on $[0, 1]$.

Proof. Recall that our experiment is made up of i.i.d. units $\{R_1, \dots, R_N\}$, where $R_i = (Y_i^{\text{obs}}, X_i, W_i)$ is a 3-tuple. Also recall from Section 3.2 that for every treatment unit R_i , we have a p -value \hat{p}_i , where $\hat{p}_i \sim U(0, 1)$ under the null hypothesis H_0 of no treatment effect. Therefore, for each of the unique covariate profiles in our treatment data $x \in U_X(D)$, we can compute the number of significant p -values, $N_\alpha(x) \sim \text{Binomial}(N(x), \alpha)$, for any given value of α . Recall that we assume $N(x) = n \forall x \in U_X(D)$, that $|U_X(D)| = M$, and that ϕ and Φ are the Gaussian pdf and cdf respectively. In order to arrive at the intended result on the distribution of $\sqrt{F(S_u^*)}$, we will need to make a set of interrelated observations.

Observation 1: Let us define $S_{\alpha,u}^* = \arg \max_{S_u \subseteq U_X(D)} F_\alpha(S_u)$, the highest scoring unconstrained subset of covariate profiles for a given α . From Theorem 1 we know that if the profiles are sorted $\{x_{(1)}, \dots, x_{(M)}\}$ according to priority function $\frac{N_\alpha(x)}{n}$, where $x_{(t)}$ has the t^{th} highest priority, then

$$\begin{aligned} S_{\alpha,u}^* &\in \{\{x_{(1)}, \dots, x_{(t)}\} \mid t \in \{1, \dots, M\}\} \\ &= \{x \mid N_\alpha(x) > t(\alpha)\}. \end{aligned}$$

Essentially, $S_{\alpha,u}^*$ will consist of all and only those profiles x with $N_\alpha(x)$ above some threshold $t(\alpha)$. Because $N_\alpha(x) \sim \text{Binomial}(n, \alpha)$ under H_0 , we can write $t(\alpha) = n\alpha + Z\sqrt{n\alpha(1-\alpha)}$ for some constant Z , allowing the threshold to represent Z -standard deviations above the expected number of significant p -values. Therefore, for given values of α and Z , the event that a given profile x will be included in $S_{\alpha,u}^*$ can be defined as

$$\begin{aligned} \mathbb{1}_{\{x \in U_X(S_{\alpha,u}^*)\}} &\sim \text{Bernoulli}\left(\mathbb{P}\left[N_\alpha(x) \geq n\alpha + Z\sqrt{n\alpha(1-\alpha)}\right]\right) \\ &\xrightarrow{d} \text{Bernoulli}(1 - \Phi(Z)), \end{aligned} \tag{17}$$

as $n \rightarrow \infty$; and consequently we also have

$$|U_X(S_{\alpha,u}^*)| \xrightarrow{d} \text{Binomial}(M, 1 - \Phi(Z)). \tag{18}$$

To close, from this observation, for fixed α and Z , we have the asymptotic distribution governing the event that an individual covariate profile will be included in the detected subset $S_{\alpha,u}^*$ and consequently the asymptotic distribution over the number of profiles to be included.

Observation 2: From (17) we also have $N_\alpha(x) \mid x \in U_X(S_{\alpha,u}^*) \sim \text{TruncatedBinomial}(n, \alpha, Z)$; for the covariate profiles included in $S_{\alpha,u}^*$, the observed number of significant p -values follow a truncated binomial distribution. Moreover, for given values of α and Z , as $n \rightarrow \infty$,

$$\sqrt{n} \left(\frac{N_\alpha(x)}{n} - \alpha \right) \Big| x \in U_X(S_{\alpha,u}^*) \xrightarrow{d} \text{TruncatedGaussian}(0, \alpha(1-\alpha), Z), \tag{19}$$

whose expected value is $\frac{\phi(Z)}{1-\Phi(Z)}\sqrt{\alpha(1-\alpha)}$ and variance is $\alpha(1-\alpha)V(Z)$, where $V(Z) < 1$ is the variance reduction from a truncated Gaussian, $V(Z) = 1 + \frac{Z\phi(Z)}{1-\Phi(Z)} - \left(\frac{\phi(Z)}{1-\Phi(Z)}\right)^2$. To

close, from this observation, for fixed α and Z , we obtain the asymptotic distribution governing the number of significant p -values for covariate profiles in the detected subset $S_{\alpha,u}^*$.

Observation 3: We can write

$$\frac{N_\alpha(S_{\alpha,u}^*)}{N(S_{\alpha,u}^*)} = \frac{\sum_{x \in U_X(S_{\alpha,u}^*)} N_\alpha(x)}{n |U_X(S_{\alpha,u}^*)|},$$

which when combined with the asymptotic distributions that govern the behaviors of profiles included in $S_{\alpha,u}^*$ (from Observations 1 and 2) we can conclude

$$\begin{aligned} \frac{\sqrt{N(S_{\alpha,u}^*)} \left(\frac{N_\alpha(S_{\alpha,u}^*)}{N(S_{\alpha,u}^*)} - \alpha \right)}{\sqrt{2\alpha(1-\alpha)}} - \sqrt{\frac{M\phi(Z)^2}{2(1-\Phi(Z))}} &= \sqrt{F_\alpha^{NA}(S_{\alpha,u}^*)} - \sqrt{\frac{M\phi(Z)^2}{2(1-\Phi(Z))}} \\ &\xrightarrow{d} \text{Gaussian} \left(0, \frac{V(Z)}{2} \right), \end{aligned} \quad (20)$$

by the Central Limit Theorem. To close, from this observation, for fixed α and Z , we have the asymptotic distribution that governs the score function for the detected subset $S_{\alpha,u}^*$.

Observation 4: While Observation 3 provides the distribution of the score function for the detected subset optimized over Z , the distribution is still defined for a fixed α . This last observation will address the supremum over α . To begin, for a given subset S , we can collect all its (treatment unit) p -values: $P_S = \{\hat{p}_i \mid x_i \in S\}$ where $|P_S| = n_s$ and $\hat{p}_i \sim U(0,1)$ under H_0 . Moreover, if we let $P_{n_s}(\alpha) = \frac{1}{n_s} \sum_{\hat{p}_i \in P_S} \mathbb{1}_{\{\hat{p}_i \leq \alpha\}}$, then $\mathbb{U}_{n_s}(\alpha) = \frac{\sqrt{n_s}(P_{n_s}(\alpha) - \alpha)}{\sqrt{\alpha(1-\alpha)}}$ is a normalized uniform empirical process, indexed by $\alpha \in (0,1)$. Next let $\mathbb{W}_{n_s}(\alpha_{\min}, \alpha_{\max}) = \sup_{\alpha \in [\alpha_{\min}, \alpha_{\max}]} |\mathbb{U}_{n_s}(\alpha)|$, be the supremum over the absolute value of the normalized uniform empirical process, restricted to $[\alpha_{\min}, \alpha_{\max}]$ in the interior of $(0,1)$. Recognize that $\sqrt{F_\alpha^{NA}(S)}$ is a scaled version of $|\mathbb{U}_{n_s}(\alpha)|$, and therefore

$$\begin{aligned} \sqrt{F^{NA}(S)} &= \sup_{\alpha \in [\alpha_{\min}, \alpha_{\max}]} \sqrt{F_\alpha^{NA}(S)} \\ &\propto \mathbb{W}_{n_s}(\alpha_{\min}, \alpha_{\max}) \\ &\xrightarrow{d} \mathbb{W}(\alpha_{\min}, \alpha_{\max}) \\ &= \sup_{\alpha \in [\alpha_{\min}, \alpha_{\max}]} \frac{|B(\alpha)|}{\sqrt{\alpha(1-\alpha)}}, \end{aligned} \quad (21)$$

where $B(\alpha)$ is the Brownian bridge on $[0,1]$. We consider the supremum over $[\alpha_{\min}, \alpha_{\max}]$ in the interior of $[0,1]$ because if left unrestricted, $\mathbb{W}_{n_s}(0,1)$ increases with n_s , and $\mathbb{W}(0,1)$ becomes arbitrarily large [37]. So to close, from this observation, for fixed Z but supremum over quantiles α , we know that the score function for any subset S follows a normalized uniform empirical process.

If we take all four observations together with the definition of $F^{NA}(S_u^*)$, we obtain

$$\begin{aligned}
\max_{S_u \subseteq U_X(D)} \sqrt{F^{NA}(S_u)} &= \max_{S_u \subseteq U_X(D), \alpha \in [\alpha_{\min}, \alpha_{\max}]} \sqrt{F_{\alpha}^{NA}(S_u)} \\
&= \max_{Z, \alpha \in [\alpha_{\min}, \alpha_{\max}]} \frac{\sqrt{N(S_u^*) \left(\frac{N_{\alpha}(S_u^*)}{N(S_u^*)} - \alpha \right)}}{\sqrt{2\alpha(1-\alpha)}} \\
&\xrightarrow{d} \max_{Z, \alpha \in [\alpha_{\min}, \alpha_{\max}]} \text{Gaussian} \left(\sqrt{\frac{M\phi(Z)^2}{2(1-\Phi(Z))}}, \frac{V(Z)}{2} \right) \\
&\xrightarrow{d} \max_Z \left(\sqrt{\frac{M\phi(Z)^2}{2(1-\Phi(Z))}} + \mathbb{W}(\alpha_{\min}, \alpha_{\max}) \sqrt{\frac{V(Z)}{2}} \right) \\
&< 0.45\sqrt{M} + \frac{\mathbb{W}(\alpha_{\min}, \alpha_{\max})}{\sqrt{2}},
\end{aligned}$$

where the last inequality follows from $\max_Z \sqrt{\frac{\phi(Z)^2}{2(1-\Phi(Z))}} < 0.45$ and $\max_Z V(Z) < 1$.

Now that we have this asymptotic behavior of $F^{NA}(S_u^*)$, we recall two results. First, under H_0 , for our score function of choice in the main text, $F^{BJ}(S) \xrightarrow{a.s.} F^{NA}(S) \forall S$ (Proposition 2). Second, by Proposition 3, all other score functions we reference in Appendix A are maximizations over continuous and monotonic transformations of $F_{\alpha}^{NA}(S)$. Therefore the limiting distribution of $\max_{S \subseteq U_X(D)} F(S)$ under H_0 for all our score functions can simply be derived from this specific result for $F^{NA}(S)$, mutatis mutandis. \square

Theorem 2. *Under H_0 defined in (12), let $N(x) = n \forall x \in U_X(D)$ and fix Type-I error rate $\delta > 0$, then there exists a critical value $h(\delta)$ such that*

$$\lim_{n \rightarrow \infty} P_{H_0} \left(\max_{S \in \text{Rect}} F(S) > h(\delta) \right) \leq \delta.$$

Proof. For false positive rate $\delta > 0$, we first define $w(\delta)$, which returns w such that $P(\mathbb{W}(\alpha_{\min}, \alpha_{\max}) > w) = \delta$. [37] show that as $w \rightarrow \infty$,

$$P(\mathbb{W}(\alpha_{\min}, \alpha_{\max}) > w) = \left(w \log \left(\frac{\alpha_{\max}(1 - \alpha_{\min})}{\alpha_{\min}(1 - \alpha_{\max})} \right) + O(w^{-1}) \right) \phi(w), \quad (22)$$

and also note that we can use the tables of [28] to obtain the tail probability in (22) exactly. Next, we define $h(\delta) = \left(0.45\sqrt{M} + \frac{w(\delta)}{\sqrt{2}} \right)^2$. As $n \rightarrow \infty$,

$$P_{H_0} \left(\max_{S \in \text{Rect}} F(S) > h(\delta) \right) \leq P_{H_0} \left(\max_{S \subseteq U_X(D)} \sqrt{F^{NA}(S)} > 0.45\sqrt{M} + \frac{w(\delta)}{\sqrt{2}} \right) \quad (23)$$

$$\begin{aligned}
&\leq P \left(0.45\sqrt{M} + \frac{\mathbb{W}(\alpha_{\min}, \alpha_{\max})}{\sqrt{2}} > 0.45\sqrt{M} + \frac{w(\delta)}{\sqrt{2}} \right) \quad (24) \\
&= P(\mathbb{W}(\alpha_{\min}, \alpha_{\max}) > w(\delta)) \\
&= \delta
\end{aligned}$$

where the inequality in (23) follows from the fact that the space of rectangular subsets is contained within the space of all subsets, and (24) follows from Lemma 1. \square

Given asymptotic control over the score when the null hypothesis is true, we now turn our attention to the score when the null hypothesis is false. We begin by first recognizing that for any $\alpha \in [\alpha_{\min}, \alpha_{\max}]$, $F_\alpha(S^T) \leq F(S^T) \leq F(S^*)$. The latter inequality indicates that the score of the optimal rectangular subset is lower-bounded by the score of the truly affected (rectangular) subset, because by definition, no subset achieves a higher score than S^* . The former inequality indicates that the score of the true subset evaluated at a given α lower bounds the score of the true subset maximized over all α . Consequently, under $H_1(S^T)$, the distribution of $F_\alpha(S^T)$ for any α provides a lower bound on the distribution of $F(S^T)$, and consequently $F(S^*)$. Therefore we will begin by establishing the distribution of $\sqrt{F_{\alpha^*}(S^T)}$ under $H_1(S^T)$, for the specific $\alpha^* = \arg \max_{\alpha} \frac{(\beta(\alpha) - \alpha)^2}{2\alpha(1 - \alpha)}$.

Lemma 2. *Under $H_1(S^T)$ defined in (12), let $N(x) = n \forall x \in U_X(D)$, and consider $F_{\alpha^*}(S^T)$ for $\alpha^* = \arg \max_{\alpha \in [\alpha_{\min}, \alpha_{\max}]} \frac{(\beta(\alpha) - \alpha)^2}{2\alpha(1 - \alpha)}$ and $\beta^* = \beta(\alpha^*)$. Then as $n \rightarrow \infty$,*

$$\sqrt{F_{\alpha^*}(S^T)} - O\left(\sqrt{kMn}\right) \xrightarrow{d} \text{Gaussian}\left(0, \sigma_{\alpha^*\beta^*}^2\right),$$

where $\sigma_{\alpha^*\beta^*}^2 > 0$ does not depend on k , M , or n .

Proof. First, recognize that $N(S^T) = kMn$ and that $N_{\alpha^*}(S^T) \sim \text{Binomial}(N(S^T), \beta^*)$. Therefore, we have the following:

$$\begin{aligned} F_{\alpha^*}^{NA}(S^T) &= \frac{(N_{\alpha^*}(S^T) - N(S^T)\alpha^*)^2}{2N(S^T)\alpha^*(1 - \alpha^*)} \\ &= \frac{N(S^T) \left(\frac{N_{\alpha^*}(S^T)}{N(S^T)} - \alpha^* \right)^2}{2\alpha^*(1 - \alpha^*)} \\ &= \frac{kMn (\hat{\beta}^* - \alpha^*)^2}{2\alpha^*(1 - \alpha^*)}. \end{aligned}$$

Next, by the Central Limit Theorem we have

$$\sqrt{n}(\hat{\beta}^* - \beta^*) \xrightarrow{d} \text{Gaussian}\left(0, \frac{\beta^*(1 - \beta^*)}{kM}\right),$$

and therefore, by the delta method we also have

$$\sqrt{n} \left(g(\hat{\beta}^*) - g(\beta^*) \right) \xrightarrow{d} \text{Gaussian}\left(0, \frac{\beta^*(1 - \beta^*)}{kM} g'(\beta^*)^2\right).$$

If we allow $g(b) = \sqrt{\frac{kM}{2\alpha^*(1 - \alpha^*)}}(b - \alpha^*)$, we then finally have

$$\sqrt{F_{\alpha^*}^{NA}(S^T)} - \sqrt{\frac{kMn(\beta^* - \alpha^*)^2}{2\alpha^*(1 - \alpha^*)}} \xrightarrow{d} \text{Gaussian}\left(0, \frac{\beta^*(1 - \beta^*)}{2\alpha^*(1 - \alpha^*)}\right).$$

From Proposition 2 we know that, for our score function of choice in the main text, $F_{\alpha^*}^{BJ}(S)$ is bounded above and below by either $F_{\alpha^*}^{NA}(S)$ or a constant times $F_{\alpha^*}^{NA}(S) \forall S$. Second,

by Proposition 3 all other functions F_α we reference in Appendix A are continuous and monotonic transformations of $F_\alpha^{NA}(S)$. Therefore, the corresponding limiting distributions under $H_1(S^T)$ for all functions $F_{\alpha^*}(S)$ can simply be derived from this result for $F_\alpha^{NA}(S)$, mutatis mutandis. \square

Theorem 3. *Under $H_1(S^T)$ defined in (12), let $N(x) = n \forall x \in U_X(D)$ and critical value $h(\delta)$ be set for the same fixed Type-I error rate $\delta > 0$ as in Theorem 2, then*

$$\lim_{n \rightarrow \infty} P_{H_1} \left(\max_{S \in Rect} F(S) > h(\delta) \right) = 1.$$

Proof. First, we note that under $H_1(S^T)$

$$F_{\alpha^*}(S^T) \leq F(S^*),$$

because the detected subset $S^* = \arg \max_{S \in Rect, \alpha \in [\alpha_{\min}, \alpha_{\max}]} F_\alpha(S)$, while $S^T \in Rect$ and $\alpha^* \in [\alpha_{\min}, \alpha_{\max}]$. Now that we have a lower bound on $F(S^*)$ under $H_1(S^T)$, we consider the critical value $h(\delta)$ for fixed Type-I error rate $\delta > 0$, and F^{NA} or F^{BJ} score functions.

$$\begin{aligned} P_{H_1}(F(S^*) > h(\delta)) &\geq P_{H_1}(F_{\alpha^*}(S^T) > h(\delta)) \\ &= P_{H_1} \left(F_{\alpha^*}(S^T) > \left(0.45\sqrt{M} + \frac{w(\delta)}{\sqrt{2}} \right)^2 \right) \end{aligned} \quad (25)$$

$$\begin{aligned} &= P_{H_1} \left(F_{\alpha^*}(S^T) > \left(0.45\sqrt{M} + O(1) \right)^2 \right) \\ &= P_{H_1} \left(\left(O(\sqrt{kMn}) + Z\sigma_{\alpha^*\beta^*}^2 \right)^2 > \left(0.45\sqrt{M} + O(1) \right)^2 \right), \end{aligned} \quad (26)$$

where $Z \sim \text{Gaussian}(0, 1)$, (25) follows from Theorem 2, and (26) follows from Lemma 2. For $n \rightarrow \infty$ and constant k and M , we know that the lhs of (26) goes to ∞ while the rhs does not, and thus $P_{H_1}(F(S^*) > h(\delta)) \rightarrow 1$. Finally, by Proposition 3 all other score functions we reference in Appendix A are maximizations over continuous and monotonic transformations of the continuous function $F_\alpha^{NA}(S)$; therefore, this result will hold mutatis mutandis for these transformations. \square

B.3 Subset Correctness

In this section, we are still interested in studying the properties of our framework under $H_1(S^T)$. However, we are now concerned about the correctness of the detected subset S^* : our objective is for S^* to exactly match S^T . If x is a data element, i.e., one of the M unique covariate profiles in the data; $U_X(D)$ is the collection of these data elements, i.e., $U_X(D) = \{x_1, \dots, x_M\}$; and both $U_X(S^*), U_X(S^T) \subseteq U_X(D)$. The results in this section are general, and are therefore applicable to an unconstrained (or constrained) S^T ; therefore S^* and α^* will refer to the joint maximization of subsets and α values over the unconstrained (or constrained) space in which S^T is defined. We begin building our theory by demonstrating that the score function of interest can be re-written as an additive function if we condition on the value of the null and alternative hypothesis parameters α and $\beta(\alpha)$. More specifically,

the score of a subset S can be decomposed into the sum of contributions (measured by a function ω) from each individual covariate profile x contained within the subset. For example, with respect to F^{BJ} , $\omega^{BJ}(\alpha, \beta, N_\alpha(x), N(x)) = C_{\alpha,\beta}^1 N_\alpha(x) + C_{\alpha,\beta}^2 N(x)$, where each C is only a function of α and β , and therefore constant with respect to $N_\alpha(x)$ and $N(x)$.

Lemma 3. $F(S)$ can be written as $\max_{\alpha,\beta} \sum_{x \in U_X(S)} \omega(\alpha, \beta, N_\alpha(x), N(x))$, for $\alpha, \beta \in (0, 1)$ representing quantile values of the control and treatment potential outcomes distributions respectively.

Proof. First we note that from the derivations of $F_\alpha^{BJ}(S)$ and $F_\alpha^{NA}(S)$ in Appendix A, that if we do not set $\beta = \beta_{\text{mle}}(S)$ but instead treat $\beta \in (0, 1)$ as a given quantity, then

$$\begin{aligned}
F^{BJ}(S) &= \max_{\alpha,\beta} F_{\alpha,\beta}^{BJ}(S) \\
&= \max_{\alpha,\beta} N_\alpha(S) \log\left(\frac{\beta}{\alpha}\right) + (N(S) - N_\alpha(S)) \log\left(\frac{1-\beta}{1-\alpha}\right) \\
&= \max_{\alpha,\beta} N_\alpha(S) \log\left(\frac{\beta(1-\alpha)}{\alpha(1-\beta)}\right) + N(S) \log\left(\frac{1-\beta}{1-\alpha}\right) \\
&= \max_{\alpha,\beta} \log\left(\frac{\beta(1-\alpha)}{\alpha(1-\beta)}\right) \left(\sum_{x \in U_X(S)} N_\alpha(x)\right) + \log\left(\frac{1-\beta}{1-\alpha}\right) \left(\sum_{x \in U_X(S)} N(x)\right) \\
&= \max_{\alpha,\beta} \sum_{x \in U_X(S)} \log\left(\frac{\beta(1-\alpha)}{\alpha(1-\beta)}\right) N_\alpha(x) + \log\left(\frac{1-\beta}{1-\alpha}\right) N(x) \\
&= \max_{\alpha,\beta} \sum_{x \in U_X(S)} C_{\alpha,\beta}^{BJ_1} N_\alpha(x) + C_{\alpha,\beta}^{BJ_2} N(x) \\
&= \max_{\alpha,\beta} \sum_{x \in U_X(S)} \omega^{BJ}(\alpha, \beta, N_\alpha(x), N(x))
\end{aligned}$$

$$\begin{aligned}
F^{NA}(S) &= \max_{\alpha,\beta} F_{\alpha,\beta}^{NA}(S) \\
&= \max_{\alpha,\beta} \frac{N_\alpha(S)(\beta - \alpha)}{\alpha(1 - \alpha)} + \frac{N(S)(\alpha^2 - \beta^2)}{2\alpha(1 - \alpha)} \\
&= \max_{\alpha,\beta} \frac{(\beta - \alpha)}{\alpha(1 - \alpha)} \left(\sum_{x \in U_X(S)} N_\alpha(x)\right) + \frac{(\alpha^2 - \beta^2)}{2\alpha(1 - \alpha)} \left(\sum_{x \in U_X(S)} N(x)\right) \\
&= \max_{\alpha,\beta} \sum_{x \in U_X(S)} \frac{(\beta - \alpha)}{\alpha(1 - \alpha)} N_\alpha(x) + \frac{(\alpha^2 - \beta^2)}{2\alpha(1 - \alpha)} N(x) \\
&= \max_{\alpha,\beta} \sum_{x \in U_X(S)} C_{\alpha,\beta}^{NA_1} N_\alpha(x) + C_{\alpha,\beta}^{NA_2} N(x) \\
&= \max_{\alpha,\beta} \sum_{x \in U_X(S)} \omega^{NA}(\alpha, \beta, N_\alpha(x), N(x))
\end{aligned}$$

where all the $C_{\alpha,\beta}$'s are constants with respect to given values of α, β . □

We now have that the score of a subset S can be decomposed into the sum of contributions (measured by a function ω) from each individual element contained within the subset. Next, we seek to demonstrate some important properties of the ω functions. More specifically, ω is a concave function with respect to β , which has two roots and a unique maximum.

Lemma 4. $\omega^{NA}(\alpha, \beta, N_\alpha(x), N(x))$ is concave with respect to β , maximized at $\beta_{mle}(x) = \frac{N_\alpha(x)}{N(x)}$, and has two roots $(\beta_{\min}(x), \beta_{\max}(x))$.

Proof. Firstly,

$$\begin{aligned} \frac{\partial \omega^{NA}(\alpha, \beta, N_\alpha(x), N(x))}{\partial \beta} &= \frac{N_\alpha(x) - N(x)\beta}{\alpha(1 - \alpha)} \\ &= -\frac{N(x)}{\alpha(1 - \alpha)}\beta + \frac{N_\alpha(x)}{\alpha(1 - \alpha)} \end{aligned} \quad (27)$$

$$\begin{aligned} (\text{set}) \quad 0 &= -\frac{N(x)}{\alpha(1 - \alpha)}\beta + \frac{N_\alpha(x)}{\alpha(1 - \alpha)} \\ 0 &= -N(x)\beta + N_\alpha(x) \\ \beta &= \frac{N_\alpha(x)}{N(x)}, \end{aligned} \quad (28)$$

(27) shows that the first derivative is the equation of a line, with a negative slope, and (28) shows that this line has one root at $\frac{N_\alpha(x)}{N(x)}$. This implies ω^{NA} is concave with respect to β , with at most two roots which we will refer to as $\beta_{\min}(x)$ and $\beta_{\max}(x)$, and is maximized at $\frac{N_\alpha(x)}{N(x)}$. \square

We now show the same result for ω^{BJ} .

Lemma 5. $\omega^{BJ}(\alpha, \beta, N_\alpha(x), N(x))$ is concave with respect to β , maximized at $\beta_{mle}(x) = \frac{N_\alpha(x)}{N(x)}$, and has two roots $(\beta_{\min}(x), \beta_{\max}(x))$.

Proof.

$$\begin{aligned} \frac{\partial \omega^{BJ}(\alpha, \beta, N_\alpha(x), N(x))}{\partial \beta} &= \frac{N_\alpha(x) - N(x)\beta}{\beta(1 - \beta)} \\ (\text{set}) \quad 0 &= \frac{N_\alpha(x) - N(x)\beta}{\beta(1 - \beta)} \\ 0 &= N_\alpha(x) - N(x)\beta \\ \beta &= \frac{N_\alpha(x)}{N(x)} \end{aligned}$$

shows that ω^{BJ} is maximized (if it is concave) at $\frac{N_\alpha(x)}{N(x)}$ and has at most two roots, which we will refer to as $\beta_{\min}(x)$ and $\beta_{\max}(x)$. Additionally,

$$\begin{aligned} \left. \frac{\partial^2 \omega^{BJ}(\alpha, \beta, N_\alpha(x), N(x))}{\partial^2 \beta} \right|_{\beta = \frac{N_\alpha(x)}{N(x)}} &= -\left. \frac{\beta^2 N(x) + (1 - 2\beta)N_\alpha(x)}{(\beta - 1)^2 \beta^2} \right|_{\beta = \frac{N_\alpha(x)}{N(x)}} \\ &< 0 \end{aligned}$$

shows that ω^{BJ} is concave with respect to β . \square

Intuitively, $(\beta_{\min}(x), \beta_{\max}(x))$ is the interval over which ω makes a positive contribution to the score of a subset, while this contribution is maximized at $\beta_{\text{mle}}(x)$; we note that in the case of ω^{NA} and ω^{BJ} , $\beta_{\min}(x) = \alpha$. Given that we have demonstrated that ω is concave, we now demonstrate a key insight about the relationship between $r_{\max} = \beta_{\max}(x) - \alpha$ and $r_{\text{mle}} = \beta_{\text{mle}}(x) - \alpha$.

Lemma 6. *With respect to $\omega^{NA}(\alpha, \beta, N_{\alpha}(x), N(x))$, $\frac{r_{\max}(x)}{r_{\text{mle}}(x)} = 2$.*

Proof. First, by Lemma 4, we know that, with respect to β , ω^{NA} is concave and has at most two roots $(\beta_{\min}(x), \beta_{\max}(x))$. Therefore, we have the following:

$$\begin{aligned}
\omega^{NA}(\alpha, \beta, N_{\alpha}(x), N(x)) &= \frac{N_{\alpha}(x)(\beta - \alpha)}{\alpha(1 - \alpha)} + \frac{N(x)(\alpha^2 - \beta^2)}{2\alpha(1 - \alpha)} \\
(\text{set}) \ 0 &= \frac{N_{\alpha}(x)(\beta - \alpha)}{\alpha(1 - \alpha)} + \frac{N(x)(\alpha^2 - \beta^2)}{2\alpha(1 - \alpha)} \\
&= 2N_{\alpha}(x)(\beta - \alpha) + N(x)(\alpha^2 - \beta^2) \\
&= (-N(x))\beta^2 + (2N_{\alpha}(x))\beta + (-2\alpha N_{\alpha}(x) + N(x)\alpha^2) \\
\{\beta_{\min}(x), \beta_{\max}(x)\} &= \frac{-2N_{\alpha}(x) \pm \sqrt{(2N_{\alpha}(x))^2 - 4(-N(x))(-2\alpha N_{\alpha}(x) + N(x)\alpha^2)}}{-2N(x)} \\
&= \frac{-2N_{\alpha}(x) \pm \sqrt{4(N_{\alpha}(x)^2 - 2N_{\alpha}(x)N(x)\alpha + (N(x)\alpha)^2)}}{-2N(x)} \\
&= \frac{-2N_{\alpha}(x) \pm \sqrt{4(N_{\alpha}(x) - N(x)\alpha)^2}}{-2N(x)} \\
&= \frac{N_{\alpha}(x) \pm (N_{\alpha}(x) - N(x)\alpha)}{N(x)} \\
&= \{\alpha, 2\beta_{\text{mle}}(x) - \alpha\}.
\end{aligned}$$

This implies that $\beta_{\max}(x) - \alpha = 2(\beta_{\text{mle}}(x) - \alpha)$ and thus $r_{\max}(x) = 2r_{\text{mle}}(x)$, with respect to ω^{NA} . \square

We show a similar result for ω^{BJ} .

Lemma 7. *With respect to $\omega^{BJ}(\alpha, \beta, N_{\alpha}(x), N(x))$,*

$$\frac{r_{\max}(x)}{r_{\text{mle}}(x)} \begin{cases} < 2 & \text{if } \beta_{\text{mle}}(x) > \frac{1}{2} \\ = 2 & \text{if } \beta_{\text{mle}}(x) = \frac{1}{2} \\ > 2 & \text{otherwise.} \end{cases}$$

Proof. First, by Lemma 5, we know that, with respect to β , ω^{BJ} is concave and has at most two roots $(\beta_{\min}(x), \beta_{\max}(x))$. One of the solutions of ω^{BJ} must be α , so let us assume that $\beta_{\min}(x) = \alpha$; this will be true when $\beta > \alpha$, which intuitively corresponds to our case of interest: when the covariate profile contains more significant (extreme) p -values than

expected. Furthermore, we know that ω^{BJ} achieves a maximum at $\beta_{\text{mle}} = \frac{N_\alpha(x)}{N(x)}$. With these properties we can show the first case ($1 \leq \frac{r_{\text{max}}(x)}{r_{\text{mle}}(x)} < 2$) by first recognizing that trivially $\beta_{\text{mle}} \leq \beta_{\text{max}}$, and $\beta_{\text{mle}} - \alpha \leq \beta_{\text{max}} - \alpha$. To show the upper bound of the first case, it suffices to show that $\omega^{BJ}(\alpha, \beta_{\text{mle}} - \epsilon, N_\alpha(x), N(x)) \geq \omega^{BJ}(\alpha, \beta_{\text{mle}} + \epsilon, N_\alpha(x), N(x))$ for some $\epsilon > 0$. The essential implication is that the concave function ω^{BJ} increases at a slower rate (until it reaches its maximum) than it decreases. This further implies that the distance between β_{mle} and α is larger than the distance between β_{mle} and β_{max} , and therefore the desired result.

Recall from Lemma 5 that

$$\begin{aligned} \frac{\partial \omega^{BJ}(\alpha, \beta, N_\alpha(x), N(x))}{\partial \beta} &= \frac{N_\alpha(x) - N(x)\beta}{\beta(1 - \beta)} \\ &= N(x) \left[\frac{\beta_{\text{mle}}(x) - \beta}{\beta(1 - \beta)} \right], \end{aligned}$$

which means the slope of ω^{BJ} is proportional to $\frac{\beta_{\text{mle}}(x) - \beta}{\beta(1 - \beta)}$. We now compare the slope around the inflection point $\beta_{\text{mle}}(x)$, and recognize that at $\beta = \beta_{\text{mle}}(x) + \epsilon$ the slope is negative with absolute value proportional to $\frac{\epsilon}{(\beta_{\text{mle}}(x) + \epsilon)(1 - \beta_{\text{mle}}(x) - \epsilon)}$. At $\beta = \beta_{\text{mle}}(x) - \epsilon$ the slope is positive with absolute value proportional to $\frac{\epsilon}{(\beta_{\text{mle}}(x) - \epsilon)(1 - \beta_{\text{mle}}(x) + \epsilon)}$. Therefore,

$$\begin{aligned} \beta_{\text{mle}}(x) > \frac{1}{2} &\iff (\beta_{\text{mle}}(x) + \epsilon)(1 - \beta_{\text{mle}}(x) - \epsilon) < (\beta_{\text{mle}}(x) - \epsilon)(1 - \beta_{\text{mle}}(x) + \epsilon) \\ &\iff \frac{\epsilon}{(\beta_{\text{mle}}(x) + \epsilon)(1 - \beta_{\text{mle}}(x) - \epsilon)} > \frac{\epsilon}{(\beta_{\text{mle}}(x) - \epsilon)(1 - \beta_{\text{mle}}(x) + \epsilon)} \\ &\iff \frac{r_{\text{max}}(x)}{r_{\text{mle}}(x)} < 2. \end{aligned}$$

The demonstration of the remaining two conditions follow precisely the same approach above, *mutatis mutandis*. \square

Now that we have built up the necessary properties of the ω functions, we now will discuss the sufficient conditions for the detected subset to be exactly correct, $S^* = S^T$. To begin we re-introduce some additional notation:

$$\begin{aligned} r_{\text{mle}-h}^{\text{aff}} &= \max_{x \in U_X(S^T)} r_{\text{mle}}(x), \\ r_{\text{mle}-l}^{\text{aff}} &= \min_{x \in U_X(S^T)} r_{\text{mle}}(x), \\ r_{\text{mle}-h}^{\text{unaff}} &= \max_{x \notin U_X(S^T)} r_{\text{mle}}(x), \\ \eta &= \left(\frac{\sum_{x \in U_X(S^T)} N(x)}{\sum_{x \in U_X(D)} N(x)} \right), \\ \nu - \text{homogeneous} &: \frac{r_{\text{mle}-h}^{\text{aff}}}{r_{\text{mle}-l}^{\text{aff}}} < \nu, \\ \delta - \text{strong} &: \frac{r_{\text{mle}-l}^{\text{aff}}}{r_{\text{mle}-h}^{\text{unaff}}} > \delta, \\ R &: (0, 1) \mapsto (0, 1). \end{aligned}$$

More specifically, R is an invertible function such that $R: r_{\max}(x) \mapsto r_{\text{mle}}(x)$ —i.e., if R is applied to $r_{\max}(x)$ it would produce the corresponding $r_{\text{mle}}(x)$. From Lemma 6 we know that with respect to ω^{NA} , $R^{NA}(r) = \frac{r}{2}$, while from Lemma 7 we know that with respect to ω^{BJ} , $R^{BJ}(r) \leq \frac{r}{2}$ under certain conditions.

The first result we provide is a sufficient condition for guaranteeing that the detected subset includes all the elements from the true subset ($S^* \supseteq S^T$). More specifically, we show that such a condition is sufficient homogeneity of the affected data elements: for a given value ν , and any pair of affected covariate profiles ($x_i, x_j \in U_X(S^T)$), the anomalous signal $r_{\text{mle}}(x)$ observed in x_i is no more than ν times that which is observed in x_j .

Theorem 4. *Under $H_1(S^T)$ defined in (12), where $|U_X(S^T)| = t > 0$, $\exists \nu > 1$ such that if the observed effect across the t covariate profiles in S^T is ν -homogeneous, and at least 1-strong, then the highest scoring subset $S^* \supseteq S^T$.*

Proof. First, let $\{x_{(1)}, \dots, x_{(t)}\}$ be the data elements in S^T sorted by the priority function (Theorem 1) $G(x) = \frac{N_\alpha(x)}{N(x)} = \beta_{\text{mle}}(x)$. By the assumption of an observed signal that is at least 1-strong, these data elements are the t highest priority data elements. Additionally, let $\nu = \frac{r_{\text{mle}-h}^{\text{aff}}}{R(r_{\text{mle}-h}^{\text{aff}})}$. Therefore,

$$\begin{aligned}
\nu\text{-homogeneous} &\implies \nu > \frac{r_{\text{mle}-h}^{\text{aff}}}{r_{\text{mle}-l}^{\text{aff}}} \\
&\implies \frac{r_{\text{mle}-h}^{\text{aff}}}{R(r_{\text{mle}-h}^{\text{aff}})} > \frac{r_{\text{mle}-h}^{\text{aff}}}{r_{\text{mle}-l}^{\text{aff}}} \\
&\implies r_{\text{mle}-l}^{\text{aff}} > R(r_{\text{mle}-h}^{\text{aff}}) \\
&\implies R^{-1}(r_{\text{mle}-l}^{\text{aff}}) > r_{\text{mle}-h}^{\text{aff}} \\
&\implies \beta_{\max}(x_{(t)}) - \alpha > \beta_{\text{mle}}(x_{(1)}) - \alpha \\
&\implies \beta_{\max}(x_{(t)}) > \beta_{\text{mle}}(x_{(k)}) \quad (\forall k) \\
&\implies \beta_{\max}(x_{(t)}) > \beta_{\text{mle}}(S^*) \\
&\implies \omega(\alpha, \beta_{\text{mle}}(S^*), N_\alpha(x_{(t)}), N(x_{(t)})) > 0 \\
&\implies |S^*| \geq t \\
&\implies S^* \supseteq S^T.
\end{aligned}$$

Intuitively, $\beta_{\text{mle}}(x_{(t)})$ and $\beta_{\text{mle}}(x_{(1)})$ are respectively the smallest and largest β_{mle} of all the $x \in U_X(S^T)$. Furthermore, $\beta_{\text{mle}}(x_{(t)}) \leq \beta_{\text{mle}}(x_{(k)}) \leq \beta_{\max}(x_{(t)}) \forall k \in [1, t]$, which means $\beta_{\text{mle}}(S^*) \leq \beta_{\max}(x_{(t)})$ for the optimal subset S^* . Moreover, the S^* that maximizes $F_{\alpha, \beta}$ will include any covariate profile x that would make a positive contribution to the score $F_{\alpha, \beta}$ at the given value of β . Such a positive contribution occurs when the concave ω function of x is positive. At the optimal α and $\beta = \beta_{\text{mle}}(S^*)$ the ω function for each of the $\{x_{(1)}, \dots, x_{(t)}\}$ is positive because β_{\max} (the larger root of the ω functions) for each of these elements is greater than $\beta_{\text{mle}}(S^*)$. \square

Corollary 2. *From Lemma 6 we know that with respect to ω^{NA} , $\frac{r}{R(r)} = 2$. Additionally, from Lemma 7 we know that with respect to ω^{BJ} , $\frac{r}{R(r)} \leq 2$ under certain conditions. Therefore, we can conclude that at α^* , 2-homogeneity (and 1-strength) is sufficient for $S^* \supseteq S^T$*

with respect to F^{NA} ; to F^{BJ} , under some conditions; and to the other score functions described above, by Proposition 3. Essentially, if the observed excess proportions of p -values significant at α^* vary by no more than a factor of 2 across all of the affected $x \in U_X(S^T)$, then the detected subset will include all of the affected data elements.

The next result we provide is a sufficient condition for guaranteeing that the detected subset will only include elements from the true subset ($S^* \subseteq S^T$). More specifically, we show that such a condition is sufficient strength of the affected data elements; or intuitively, for a given value δ , the anomalous signals $r_{\text{mle}}(x)$ observed in every affected data element are more than $\frac{\delta}{\eta}$ -times that of the unaffected data elements.

Theorem 5. *Under $H_1(S^T)$ defined in (12), where $|U_X(S^T)| = t > 0$, $\exists \delta > 1$ such that if the observed effect across the t covariate profiles in S^T is $\frac{\delta}{\eta}$ -strong, then the highest scoring subset $S^* \subseteq S^T$.*

Proof. First, let $D = \{x_{(1)}, \dots, x_{(t)}, x_{(t+1)}, \dots, x_{(M)}\}$ be the data elements sorted by the priority function (Theorem 1) $G(x) = \frac{N_\alpha(x)}{N(x)} = \beta_{\text{mle}}(x)$. By the assumption of $\delta > 1$ (an observed signal that is at least 1-strong), $S^T = \{x_{(1)}, \dots, x_{(t)}\}$. Additionally, if $r_{\text{mle}-h}^{\text{unaff}} \leq 0$

then $S^* \subseteq S^T$, trivially. Therefore, we assume $r_{\text{mle}-h}^{\text{unaff}} > 0$. Let $\delta = \frac{R^{-1}(r_{\text{mle}-h}^{\text{unaff}})}{r_{\text{mle}-h}^{\text{unaff}}}$. Therefore,

$$\begin{aligned}
\frac{\delta}{\eta} - \text{strong} &\implies \frac{\delta}{\eta} < \frac{r_{\text{mle}-l}^{\text{aff}}}{r_{\text{mle}-h}^{\text{unaff}}} \\
\therefore &\frac{R^{-1}(r_{\text{mle}-h}^{\text{unaff}})}{\eta r_{\text{mle}-h}^{\text{unaff}}} < \frac{r_{\text{mle}-l}^{\text{aff}}}{r_{\text{mle}-h}^{\text{unaff}}} \\
\implies &R^{-1}(r_{\text{mle}-h}^{\text{unaff}}) < \left(\frac{\sum_{x \in U_X(S^T)} N(x)}{\sum_{x \in U_X(D)} N(x)} \right) r_{\text{mle}-l}^{\text{aff}} \\
&= \frac{\sum_{x \in U_X(S^T)} r_{\text{mle}-l}^{\text{aff}} N(x)}{\sum_{x \in U_X(D)} N(x)} \\
&\leq \frac{\sum_{x \in U_X(S^T)} r_{\text{mle}}(x) N(x)}{\sum_{x \in U_X(D)} N(x)} \quad \left(\text{since } r_{\text{mle}}(x) \geq r_{\text{mle}-l}^{\text{aff}} \right) \\
&\leq \frac{\sum_{x \in U_X(S^T)} r_{\text{mle}}(x) N(x) + \sum_{x \notin U_X(S^T)} r_{\text{mle}}(x) N(x)}{\sum_{x \in U_X(D)} N(x)} \\
&= \frac{\sum_{x \in U_X(D)} r_{\text{mle}}(x) N(x)}{\sum_{x \in U_X(D)} N(x)} \\
&= \frac{\sum_{x \in U_X(D)} \left(\frac{N_\alpha(x)}{N(x)} - \alpha \right) N(x)}{\sum_{x \in U_X(D)} N(x)} \\
&= \frac{\sum_{x \in U_X(D)} N_\alpha(x) - N(x)\alpha}{\sum_{x \in U_X(D)} N(x)} \\
&= \frac{\sum_{x \in U_X(D)} N_\alpha(x) - \sum_{x \in U_X(D)} N(x)\alpha}{\sum_{x \in U_X(D)} N(x)} \\
&= \frac{\sum_{x \in U_X(D)} N_\alpha(x)}{\sum_{x \in U_X(D)} N(x)} - \alpha \\
\therefore &\beta_{\max}(x_{(t+1)}) - \alpha < \beta_{\text{mle}}(D) - \alpha \\
\implies &\beta_{\max}(x_{(t+1)}) < \beta_{\text{mle}}(x_{(t)}) \\
\implies &\beta_{\max}(x_{(t+1)}) < \beta_{\text{mle}}(S^*) \\
\therefore &\omega(\alpha, \beta_{\text{mle}}(S^*), N_\alpha(x_{(t+1)}), N(x_{(t+1)})) < 0 \\
\implies &|S^*| \leq t \\
\therefore &S^* \subseteq S^T
\end{aligned}$$

Intuitively, $\beta_{\text{mle}}(x_{(t)})$ and $\beta_{\text{mle}}(x_{(t+1)})$ are respectively the smallest affected and largest unaffected β_{mle} values. Furthermore, $\beta_{\max}(x_{(t+1)}) \leq \beta_{\text{mle}}(x_{(t)})$, which means $\beta_{\max}(x_{(t+1)}) \leq \beta_{\text{mle}}(S^*)$ for the optimal subset S^* . Moreover, the S^* that maximizes $F_{\alpha, \beta}$ will not include any data element x that has $\omega \leq 0$ and thus makes a non-positive contribution to the score $F_{\alpha, \beta}$ at the given value of β . At the optimal α and $\beta = \beta_{\text{mle}}(S^*)$ the ω function for each of the $\{x_{(t+1)}, \dots, x_{(M)}\}$ are non-positive because β_{\max} (the larger root of the ω functions) for each of these elements is less than $\beta_{\text{mle}}(S^*)$. \square

Corollary 3. *From Lemma 6 we know that with respect to ω^{NA} , $\frac{R^{-1}(r)}{r} = 2$. Additionally, from Lemma 7 we know that with respect to ω^{BJ} , $\frac{R^{-1}(r)}{r} \geq 2$ under certain conditions. Therefore, we can conclude that at α^* , $\frac{2}{\eta}$ -strength is sufficient for $S^* \subseteq S^T$ with respect to F^{NA} ; to F^{BJ} , under some conditions; and to the other score functions described above, by Proposition 3. Essentially, if the observed excess proportions of p -values significant at α^* across all of the $x \in U_X(S^T)$ are at least $\frac{2}{\eta}$ times larger than the observed excess proportions for $x \notin U_X(S^T)$, then the detected subset will only include affected data elements.*

It follows from the above corollaries that 2-homogeneity and $\frac{2}{\eta}$ -strength are sufficient for $S^* = S^T$ with respect to F^{NA} ; to F^{BJ} , under some conditions; and to the other score functions described above, by Proposition 3.

Theorem 6. *Under $H_1(S^T)$ defined in, where $|U_X(S^T)| = t > 0$, let $N(x) = n \ \forall x \in U_X(D)$. If $|U_X(D)| = M$ is fixed then as $n \rightarrow \infty$, $P(S^* = S^T) \rightarrow 1$.*

Proof. From Theorems 4 and 5, there exist constants $\nu > 1$ and $\delta > 1$ such that, if the observed effect on S^T is ν -homogeneous and $\frac{\delta}{\eta}$ -strong, then $S^* = S^T$. (For example, for the F^{NA} score function, we have shown above that $\nu = \delta = 2$.) We show that, for any $\nu > 1$ and $\delta > 1$, as $n \rightarrow \infty$, the probability that the observed effect is ν -homogeneous goes to 1, and the probability that the observed effect is $\frac{\delta}{\eta}$ -strong goes to 1. Thus, as $n \rightarrow \infty$, the observed effect is ν -homogeneous and $\frac{\delta}{\eta}$ -strong with high probability for the specific ν and δ from Theorems 4 and 5, and thus $P(S^* = S^T) \rightarrow 1$.

As a first step, we show that $F^* = F(S^*)$ is maximized for some value α^* such that $\beta(\alpha^*) > \alpha^*$ and thus $\beta(\alpha^*) - \alpha^* > 0$. It follows from Lemma 2 that $F_\alpha(S^*) \rightarrow \infty$ as $n \rightarrow \infty$ if $\beta(\alpha) > \alpha$. From Lemma 1 we know that $F_\alpha(S^*)$ is upper bounded by a constant as $n \rightarrow \infty$ if $\beta(\alpha) \leq \alpha$, and this remains true when maximizing over the entire range of α values (i.e., under the null hypothesis). Thus as $n \rightarrow \infty$, the maximum score must occur for some α^* with $\beta(\alpha^*) > \alpha^*$, and we assume this value of α for the remainder of the proof.

Next, given $r_{\text{mle}}(x) = \beta_{\text{mle}}(x) - \alpha$, we show that, as $n \rightarrow \infty$, $r_{\text{mle}}(x) \rightarrow \beta(\alpha) - \alpha > 0$ for all $x \in U_X(S^T)$, and $r_{\text{mle}}(x) \rightarrow 0$ for all $x \notin U_X(S^T)$. Note that $\beta_{\text{mle}}(x) = \frac{N_\alpha(x)}{N(x)}$, where $N_\alpha(x) \sim \text{Binomial}(N(x), p)$ with $p = \beta(\alpha)$ for all $x \in U_X(S^T)$ and $p = \alpha$ for all $x \notin U_X(S^T)$, according to $H_1(S^T)$. Therefore, by the law of large numbers we can see that $\beta_{\text{mle}}(x) \rightarrow \beta(\alpha)$ for $x \in U_X(S^T)$ and $\beta_{\text{mle}}(x) \rightarrow \alpha$ for $x \notin U_X(S^T)$.

Next, we show $r_{\text{mle}-l}^{\text{aff}} \rightarrow \beta(\alpha) - \alpha$ and $r_{\text{mle}-h}^{\text{aff}} \rightarrow \beta(\alpha) - \alpha$ as $n \rightarrow \infty$. Let i be the index of elements in the set $U_X(S^T)$ and therefore $1 \leq i \leq t$. Therefore, we have

$P(|r_{\text{mle}}^i(x) - (\beta(\alpha) - \alpha)| > \epsilon) \rightarrow 0$. Thus we can see that

$$\begin{aligned}
P(|r_{\text{mle}-h}^{\text{aff}} - (\beta(\alpha) - \alpha)| > \epsilon) &= P\left(|\max_{1 \leq i \leq t} (r_{\text{mle}}^i(x) - (\beta(\alpha) - \alpha))| > \epsilon\right) \\
&\leq P\left(\max_{1 \leq i \leq t} |r_{\text{mle}}^i(x) - (\beta(\alpha) - \alpha)| > \epsilon\right) \\
&= P\left(\bigcup_{i=1}^t \{|r_{\text{mle}}^i(x) - (\beta(\alpha) - \alpha)| > \epsilon\}\right) \\
&\leq \sum_{i=1}^t P(|r_{\text{mle}}^i(x) - (\beta(\alpha) - \alpha)| > \epsilon) \\
&\rightarrow 0.
\end{aligned}$$

The last convergence is due to a fixed value of t . Using similar reasoning, we can show $r_{\text{mle}-l}^{\text{aff}} \rightarrow \beta(\alpha) - \alpha$ and therefore, $\frac{r_{\text{mle}-h}^{\text{aff}}}{r_{\text{mle}-l}^{\text{aff}}} \rightarrow \frac{\beta(\alpha)}{\beta(\alpha)} = 1$ by Slutsky's theorem. That is, for any $\nu > 1$, as $n \rightarrow \infty$, the probability that $\frac{r_{\text{mle}-h}^{\text{aff}}}{r_{\text{mle}-l}^{\text{aff}}} < \nu$, and thus that the observed effect on S^T is ν -homogeneous, goes to 1.

Next, we focus on the case where $\exists x \notin U_X(S^T)$ s.t. $r_{\text{mle}}(x) > 0$, since $S^* \subseteq S^T$ holds trivially for the case when $r_{\text{mle}}(x) \leq 0 \forall x \notin U_X(S^T)$. We now show that for a fixed M , as $n \rightarrow \infty$, $r_{\text{mle}-h}^{\text{unaff}} \rightarrow 0^+$. Let j be the index of elements in the set $x \notin U_X(S^T)$, therefore, $1 \leq j \leq M - t$. We have $r_{\text{mle}}^j(x) \rightarrow 0$, that is, $P(r_{\text{mle}}^j(x) > \epsilon) \rightarrow 0$ for all $1 \leq j \leq M - t$. Thus we can see that

$$\begin{aligned}
P(r_{\text{mle}-h}^{\text{unaff}} > \epsilon) &= P\left(\max_{1 \leq j \leq M-t} r_{\text{mle}}^j(x) > \epsilon\right) \\
&= P\left(\bigcup_{j=1}^{M-t} \{r_{\text{mle}}^j(x) > \epsilon\}\right) \\
&\leq \sum_{j=1}^{M-t} P(r_{\text{mle}}^j(x) > \epsilon) \\
&\rightarrow 0.
\end{aligned}$$

Again, the last convergence above is due to $M - t$ being fixed. Given that we have shown $r_{\text{mle}-h}^{\text{unaff}} \rightarrow 0^+$, and $r_{\text{mle}-l}^{\text{aff}} \rightarrow \beta(\alpha) - \alpha > 0$, this implies that $\frac{r_{\text{mle}-l}^{\text{aff}}}{r_{\text{mle}-h}^{\text{unaff}}} \rightarrow \infty$ as $n \rightarrow \infty$. Thus for any finite value of $\delta > 1$, and for $\eta = \frac{t}{M} > 0$, the probability that $\frac{r_{\text{mle}-l}^{\text{aff}}}{r_{\text{mle}-h}^{\text{unaff}}} > \frac{\delta}{\eta}$, and thus that the observed effect is $\frac{\delta}{\eta}$ -strong, goes to 1 as $n \rightarrow \infty$. \square

Theorem 7. Under $H_1(S^T)$ defined in (12), where $|U_X(S^T)| = t > 0$ and $S^T \in \text{Rect}$, let $N(x) = n \forall x \in U_X(D)$. Assume $|U_X(D)| = M$ is fixed. Let \hat{S}^* denote the subset returned by a given iteration of the TESS algorithm, which was initialized to some subset $S_0 \in \text{Rect}$, such that $S^T \cap S_0 \neq \emptyset$. Then as $n \rightarrow \infty$, $P(\hat{S}^* = S^T) \rightarrow 1$.

Proof. We represent $S^T = v^{1T} \times \dots \times v^{dT}$, where $v^{jT} \subseteq V^j$, and $S_0 = v_0^1 \times \dots \times v_0^d$, where $v_0^j \subseteq V^j$. Assume without loss of generality that TESS optimizes over modes $\{1, 2, \dots, d\}$

in order to obtain $S_1 = v_1^1 \times \dots \times v_1^d$, where $v_1^j \subseteq V^j$, then optimizes over modes $\{1, 2, \dots, d\}$ in order again to obtain $S_2 = v_2^1 \times \dots \times v_2^d$, where $v_2^j \subseteq V^j$. We will show that the following hold w.h.p.: (1) $S_1 \subseteq S^T$, i.e., $v_1^j \subseteq v^{jT} \forall j$; (2) $S_2 = S^T$, i.e., $v_2^j = v^{jT} \forall j$; and (3) $\hat{S}^* = S_2$.

First, we consider the optimization over the first mode for S_1 , starting from S_0 and thus finding the subset $S = v_1^1 \times v_0^2 \times \dots \times v_0^d$ which maximizes $F(S)$ for fixed $v_0^2 \dots v_0^d$. Consider the “slices” $x_m = \{v_m\} \times v_0^2 \times \dots \times v_0^d$, where $v_m \in V^1$. For $v_m \notin v^{1T}$, we know that $x_m \cap S^T = \emptyset$, and thus $r_{\text{mle}}(x_m) \rightarrow 0$ as $n \rightarrow \infty$. For $v_m \in v^{1T}$, $x_m \cap S^T$ includes some non-zero proportion ρ_m of cells for which $r_{\text{mle}}(x) \rightarrow \beta(\alpha^*) - \alpha^*$ as $n \rightarrow \infty$, and thus $r_{\text{mle}}(x_m) \rightarrow \rho_m(\beta(\alpha^*) - \alpha^*)$ as $n \rightarrow \infty$. This implies that the observed effect on the x_m is $\frac{\delta}{\eta}$ -strong w.h.p. for any $\delta > 1$ and thus for the specific δ from Theorem 5. Hence $v_1^1 \subseteq v^{1T}$ w.h.p. Identical logic can be used to show $v_1^j \subseteq v^{jT}$ w.h.p. for each j from 2 to d in turn, and thus $S_1 \subseteq S^T$ w.h.p.

Now we consider the optimization over the first mode for S_2 , starting from S_1 and thus finding the subset $S = v_2^1 \times v_1^2 \times \dots \times v_1^d$ which maximizes $F(S)$ for fixed $v_1^2 \dots v_1^d$. Consider the “slices” $x_m = \{v_m\} \times v_1^2 \times \dots \times v_1^d$, where $v_m \in V^1$. For $v_m \notin v^{1T}$, we know that $x_m \cap S^T = \emptyset$, and thus $r_{\text{mle}}(x_m) \rightarrow 0$ as $n \rightarrow \infty$. For $v_m \in v^{1T}$, since $v_1^j \subseteq v^{jT}$ for $j \in \{2, \dots, d\}$, we know $x_m \subseteq S^T$, and thus $r_{\text{mle}}(x_m) \rightarrow \beta(\alpha^*) - \alpha^*$ as $n \rightarrow \infty$. This implies that the observed effect on the x_m is $\frac{\delta}{\eta}$ -strong and ν -homogeneous w.h.p. for any $\delta > 1$ and $\nu > 1$, and thus for the specific δ and ν from Theorems 4 and 5. Hence $v_2^1 = v^{1T}$ w.h.p. Identical logic can be used to show $v_2^j = v^{jT}$ w.h.p. for each j from 2 to d in turn, and thus $S_2 = S^T$ w.h.p.

Finally, identical logic can be used to show w.h.p. that, for any mode j , S_2 is the subset $S = v^j \times v_2^{-j}$ which maximizes $F(S)$ for fixed v_2^{-j} . Thus no optimization over any mode can further increase $F(S)$, and $\hat{S}^* = S_2 = S^T$ w.h.p. \square